Survey of Ophthalmology xxx (xxxx) xxx

Contents lists available at ScienceDirect

Survey of Ophthalmology

journal homepage: www.elsevier.com/locate/survophthal

Review article

Choroidal biomarkers in age-related macular degeneration

Elham Sadeghi, MD [a], Nicola Valsecchi, MD [a,b,c], Elham Rahmanipour, MD [d], Mahsa Ejlalidiz, MD [e], Nasiq Hasan, MD [a], Kiran Kumar Vupparaboina, PhD [a], Mohammed Nasar Ibrahim, PhD [a], Mohammed Abdul Rasheed [f], Jiwon Baek [g,h], Danilo Iannetta, MD [i], Jay Chhablani, MD [a,*]

[a] University of Pittsburgh, School of Medicine, Pittsburgh, PA, USA
[b] Ophthalmology Unit, Dipartimento di Scienze Mediche e Chirurgiche, Alma Mater Studiorum University of Bologna, Bologna, Italy
[c] IRCCS Azienda Ospedaliero-Universitaria di Bologna, Bologna, Italy
[d] Immunology Research Center, Mashhad University of Medical Science, Mashhad, Iran
[e] Research Institute of Ophthalmology and Vision Science, Shahid Beheshti University of Medical Science, Tehran, Iran
[f] School of Optometry and Vision Sciences, University of Waterloo, Ontario, Canada
[g] Department of Ophthalmology, Bucheon St. Mary's Hospital, College of Medicine, The Catholic University of Korea, Bucheon, Gyeonggi-do, Republic of Korea
[h] Department of Ophthalmology, College of Medicine, The Catholic University of Korea, Seoul, Republic of Korea
[i] University of Rome La Sapienza Department of Organs of Sense, Rome, Italy

ARTICLE INFO

Keywords:
Age-related macular degeneration
Choroidal biomarker
Choroidal thickness
Choroidal vascularity
Choroidal volume
Choroidal vascularity index
Choroidal contour analysis
Choroidal vessel layer thickness analysis

ABSTRACT

Age-related macular degeneration (AMD) is the leading cause of central visual impairment in the elderly. The exact pathophysiological mechanisms for AMD remain uncertain. Several studies suggest that choroidal abnormalities and alterations are critical in AMD progression. The transition from manual to automated segmentation and binarization techniques has resulted in accurate and precise measurements of different choroidal parameters. These qualitative and quantitative parameters, known as choroidal imaging biomarkers, have advanced from basic vertical subfoveal choroidal thickness to more intricate 3-dimensional choroidal reconstruction methods in the last decade. Therefore, a comprehensive evaluation of choroidal metrics may investigate valuable insights into AMD, potentially guiding the future development of customized therapeutic strategies and personalized patient care in AMD management. We describe the role of different choroidal biomarkers in evaluating patients with AMD and their contribution to management.

1. Introduction

Globally, age-related macular degeneration (AMD) is the leading cause of irreparable central visual impairment in the elderly. It is seen in patients 50 years and older, and its prevalence significantly increases with advanced age. The pooled annual incidence of any late AMD is 1.4 per 1000 individuals. [111] According to available data, there will be a rise to 288 million patients with AMD by 2040 [127]. AMD is primarily categorized into dry (non-exudative or atrophic) and wet (exudative or neovascular) forms. Dry AMD (dAMD) is the more common type which may initially be present as drusen beneath the retinal pigment epithelium (RPE). Drusen varies in type, size, shape, and composition. Hard drusen (or small drusen) are well-defined, spherical deposits of ≤ 63 μm and represent the sole type of drusen regarded as typical age-related occurrences. Intermediate drusen have a diameter between 63 μm to 125 μm, and soft drusen (large drusen) are greater than 125 μm in diameter. [62] Larger drusen may become confluent and form drusenoid pigment epithelial detachments (PED) that may reduce the exchange of nutrients and waste products between the photoreceptor layer and choroidal blood vessels, thus accelerating degeneration and atrophy of the retina, a pathological process evident in AMD. [77] Another type is cuticular drusen that measure between 25 μm and 75 μm and tend to coalesce into larger drusen, carrying a higher risk of AMD progression. [59,191]. The deposits that accumulate in the subretinal area (above the

* Correspondence to: Department of Ophthalmology, University of Pittsburgh School of Medicine, Pittsburgh, PA, USA.
E-mail addresses: elham.sadeghi@rocketmail.com, el.sadeghi91@gmail.com (E. Sadeghi), nicola.valsecchi2@studio.unibo.it (N. Valsecchi), Elhamrahmanipour@gmail.com (E. Rahmanipour), Mahsaejlalidiz@gmail.com (M. Ejlalidiz), nasiq.imtiaz@gmail.com (N. Hasan), kiran1559@gmail.com (K.K. Vupparaboina), mohammednasari@gmail.com (M.N. Ibrahim), hcu.sahil@gmail.com (M.A. Rasheed), md.jiwon@gmail.com (J. Baek), iannettadanilo@gmail.com (D. Iannetta), jay.chhablani@gmail.com (J. Chhablani).

https://doi.org/10.1016/j.survophthal.2024.10.004
Received 2 April 2024; Received in revised form 7 October 2024; Accepted 14 October 2024
Available online 18 October 2024

RPE layer) are referred to as reticular pseudodrusen (RPD) or subretinal drusenoid deposits (SDD). These deposits have unique morphological characteristics that set them apart from other subtypes of drusen. Furthermore, they carry an elevated risk of advancing toward geographic atrophy (GA) and retinal angiomatous proliferation (RAP) [209].

Neovascular AMD (nAMD) is characterized by choroidal neovascularization (CNV) or macular neovascularization (MNV) which is newly formed blood vessels that arise from the choroid to the retina. nAMD damages the macula abruptly and severely, leading to rapid visual loss [150]. CNV can be diagnosed clinically as a greyish subretinal lesion which may be accompanied by subretinal exudation or hemorrhage. It is identified as an area of dye leakage in fluorescein angiography (FA) and indocyanine green angiography (ICGA) and an abnormal network of vessels on optical coherence tomography angiography (OCTA).

Multimodal imaging has been used to describe and characterize 3 subgroups of CNV:

- CNV type 1 (previously referred to as "occult" neovascularization), is the most prevalent type of CNV and is characterized by the presence of CNV underneath the RPE. Polypoidal choroidal vasculopathy (PCV) consists of polypoidal lesions with a network of branching neovascular vessels and is a variation of type 1 MNV, which is best detected with ICGA[58].
- CNV type 2 (also referred to as "classic" neovascularization) is defined by the existence of CNV above the RPE.
- CNV type 3 (also called RAP) is defined by aberrant vascular complexes that start within the retina [124,206].

2. Choroid and AMD

Vascular endothelial growth factors (VEGFs) are critical mediators of angiogenesis in CNV formation, and anti-VEGF therapy stands as the most effective management for neovascular AMD (nAMD); [16] however, the exact pathophysiological mechanisms for the incidence and progression of AMD remain uncertain. Several studies indicate that choroidal abnormalities and alterations are critical in AMD pathogenesis.

Anatomically, the choroid comprises 5 layers: Bruch membrane, the choriocapillaris (CC), Sattler layer (medium-sized vessels), Haller layer (large vessels), and the suprachoroidal lamina. The choroid is essential for preserving retinal health as it provides nutrition and removes waste and dead cells from the photoreceptors and outer retinal layers. Any ischemic or degenerative insult can exacerbate the progression of AMD [166,183]. Therefore, a deeper understanding of choroidal features and their role in AMD is likely to aid in identifying potential biomarkers that may further help in staging the disease, assessing treatment response, and predicting progression [16,152,195].

Imaging has become an indispensable tool in our clinical practice, especially with diseases involving the retina. Its utility in AMD has become more essential as it helps identify and measure various signs such as drusen volume, RPE alterations, neovascularization, etc. [183].

Choroidal biomarkers are objective indices that quantify variables associated with choroidal morphology or vascularity. These markers aid in prognostication and predicting the course of disease. Nevertheless, accurately identifying the condition or determining treatment outcomes based on these indices continues to pose a significant challenge. [173] Advances in ocular imaging have unveiled several choroidal biomarkers such as choroidal thickness (ChT), choroidal vascularity index (CVI), choroidal volume (CVol), choroidal vessel layer thickness analysis, and choroidal contour analysis that may aid in early detection, monitoring, and understanding the pathogenesis of AMD [57,93]. Moreover, optical coherence tomography angiography (OCTA) has become an indispensable tool in managing AMD patients, as it allows for assessing the choroidal circulation flow, vessel density, and the qualitative and quantitative characteristics of CNV. Identifying these choroidal biomarkers can significantly improve the clinical approach to early detection, prognosis, and therapeutic interventions in AMD. Therefore, we discuss potential choroidal biomarkers to introduce innovative strategies for a better approach to AMD.

3. Choroidal thickness

ChT is the most extensively researched choroidal metric, and it denotes the vertical length from the Bruch membrane to the choroid-sclera interface (CSI) [76,119]. ChT is dependent on several physiological and pathological variables and is affected by time (diurnal variation), age, gender, refraction, and ethnicity [83,112]. ChT is highly variable as significant changes have been described during measurements taken at different times of the day and changes in the object's focus. As large as 100 μm change can happen quickly after myopic defocus stimulus and up to 40 μm difference between measurements taken during the day and evening. It may also be affected by dehydration. [40; 137; 188]Abnormal ChT has also been described in several ocular and extraocular illnesses, including nAMD, Vogt-Koyanagi-Harada syndrome (VKH), PCV, and central serous chorioretinopathy (CSCR). [28]. Previous research demonstrated that peripheral myopic defocuses brought on by orthokeratology lenses, myopic anisometropia, and hemodialysis in end-stage renal disease patients can all alter ChT [74,113,192]. Subfoveal ChT (SFCT) has been investigated in numerous studies. The normal range of SFCT in different studies varied from 191.5 ± 74.2 μm to 354 ± 111 μm [76,83,120]. The substantial variability observed in SFCT readings can be attributed to factors such as age, ethnic differences, axial length discrepancies among the subjects, and the lack of universally standardized measurement methods. Consequently, determining a normal cut-off is challenging. In the Western population, Spaide and coworkers, by evaluating subjects with a mean age of 33.4 years, reported that the normal SFCT is 318 μm in the right eye and 335 μm in the left eye, whereas Manjunath and coworkers (mean age - 51.1 years), reported mean SFCT of 272 μm [118,177]. In these studies, no adjustments were made for age, gender, or axial length. A study conducted in India revealed a mean SFCT of 280.1 ± 46.5 μm in the eyes of healthy adult individuals (mean age was 42.8 ± 13.6 years, and mean axial length was 22.84 ± 0.78 mm). In the context of multivariate regression analysis, age emerged as the most influential factor impacting SFCT. The regression model indicated an estimated annual reduction in ChT of approximately 1.18 μm. [38]. Similarly, SFCT values of 261.93 ± 88.42 μm in Chinese populations and 354 ± 111 μm in Japanese populations have been reported in population-based investigations [51,83]. Additionally, a previous study documented SFCT values of 311.2 ± 45.19 μm in a sample of healthy Indian youngsters with a mean age of 11.9 years [39]. The variation in the topographic localization of the ChT measurement point is also a significant factor in choroidal measurements, as ChT decreases with increasing distance from the fovea, both nasally and temporally [38,120]. Furthermore, numerous research studies have shown that ChT decreases by approximately 12.7–15.6 μm per decade. [63,120]. There are divergent accounts regarding the correlation between gender and ChT variation. Li and colleagues discovered that ChT in men was 18 % greater than in women [112]. In contrast, no gender differences in ChT have been observed in the subgroup of healthy Indian children [36,39]. Also, a recent study reported a mean SFCT value of 206.4 ± 83.0 μm in subjects older than 75. In the context of this study, SFCT remained unaffected by gender, cardiovascular issues, classical cardiovascular risk factors, or prognostic risk scores. [8]

3.1. dAMD and GA

The variations in ChT in AMD, which are characterized by either thinning or increased thickness, are seen in different stages of AMD [90,207]. dAMD is distinguished predominantly by the manifestation of drusen and pigmentary changes. Imaging methods can be employed to

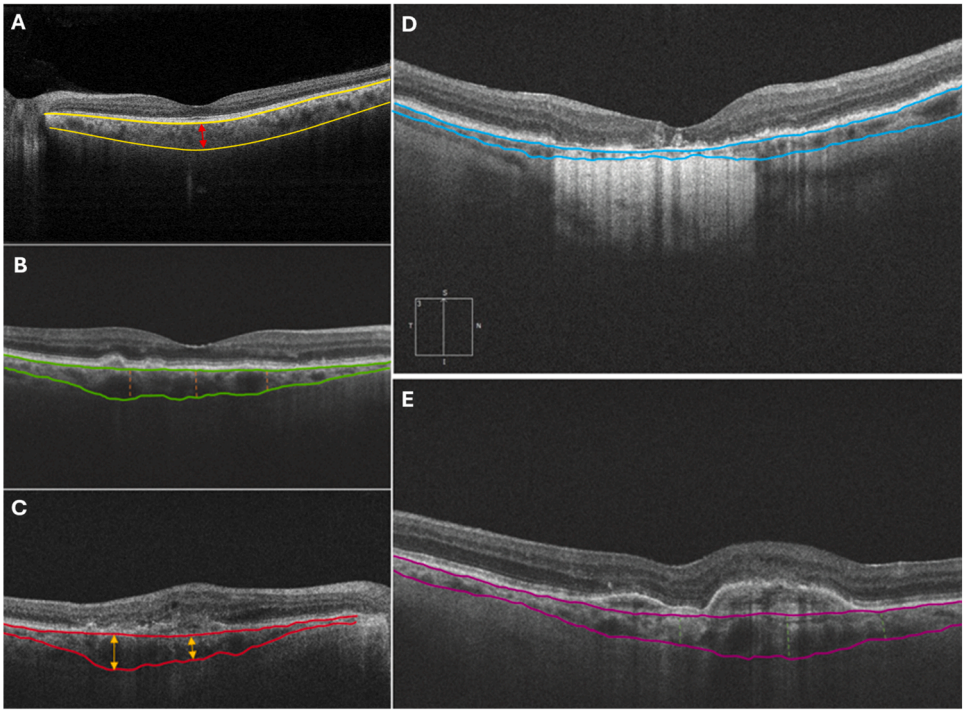

Fig. 1. This figure shows the choroidal thickness in different stages of age-related macular degeneration (AMD). Figure 1-A**:** Choroidal thickness (ChT) in the left eye of a 20-year-old healthy female subject. The two lines show the boundaries of the choroid in the Bruch membrane and the scleral-choroidal junction. The ChT in the subfoveal area (SFCT) is 295 μm, which becomes thinner through the nasal and temporal part. Figure 1-B**:** ChT in the right eye of a 65-year-old dry AMD patient. The choroid shows general thinning in the subfoveal (180 μm) and surrounding area. Figure 1-C**:** The ChT in the right eye of a 72-year-old patient with retinal angiomatous proliferation (RAP) lesion. The choroid in the area of the lesion (167 μm) is thinner than the other areas. Figure 1-D**:** The ChT in an 84-year-old patient with geographic atrophy (GA). The vertical scan of the right eye shows severe choroidal thinning especially in the area of GA (SFCT: 40 μm). **Fig1-E:** The ChT in a 71-year-old male with left eye neovascular AMD (nAMD). The choroid beneath the CNV is thicker (214 μm) than the other area.

evaluate ChT in response to the presence and type of drusen [56].

Previous studies found that there may be little to no changes in ChT in early-stage dAMD with medium-sized drusen, using OCT imaging; however, the choroid may appear thinner than usual in situations where soft drusen are present [90]. It has been demonstrated that regions with high concentrations of drusen may experience a reduction in ChT. This might result from a sustained ischemic process leading to choroidal atrophy, or it could be linked to the mechanical compression exerted by drusen on the underlying choroidal veins. [163]. Moreover, some findings suggest that drusen may be linked to choroidal circulation abnormalities.

Spaide and coworkers introduced the term “pachydrusen” as a special type of drusen with choroidal thickening. [176] They have been described in patients with dAMD and PCV. [107,170,174] According to Cheung and coworkers, ChT is independently related to the drusen subtype; thicker choroid is linked to pachydrusen, while thin choroid is linked to RPD. The underlying pathophysiology, which involves choroidal vascular insufficiency, may be reflected in choroidal thinning [34].

In significant drusen, EDI-OCT shows choroidal thinning, indicating that the underlying retina’s choroidal support has diminished [94]. Similarly, different types of drusen can influence ChT variably, with larger, confluent drusen typically associated with localized choroidal thinning; however, it has been shown that eyes with dAMD have irregular blood flow and lower blood volume compared to normal eyes, with blood flow deteriorating more as the severity of the illness increases. Several factors may contribute to the diminished blood flow observed in AMD. These include cellular depletion, CC lumen constriction, and choroidal thinning, specifically the CC layer. Additionally, reports suggest that patients diagnosed with AMD exhibit reduced levels of nitric oxide, potentially leading to vasoconstriction and hypoxia. This condition is characterized by choroidal vascular insufficiency and manifests as choroidal thinning [23,71].

A previous study by Manjunath and coworkers on 47 patients with nAMD and dAMD showed that patients with nAMD had a mean SFCT of 194.6 μm (SD, 88.4; n = 40), whereas those with dAMD, the SFCT was 213.4 μm (SD: 92.2; n = 17). Half (50.8 %) of the evaluated eyes had ChT more than one standard deviation away from the mean, whereas a small fraction (3.5 %) had ChT more than two SDs above the mean. Compared to age-adjusted normal eyes, the choroids of 33 % of the eyes were thinner. [119]. This finding may suggest that choroidal thinning contributes to AMD’s development or progression.

The late stage of dAMD, called geographic atrophy (GA), is marked by irreversible vision loss due to CC, photoreceptors, and RPE shrinkage [167]. Studies generally agree that in regions affected by GA, the choroid tends to be thinner, and it has been demonstrated that severe AMD-related GA has a remarkably lower ChT compared to the control group [115,165]. Nevertheless, patients with GA may occasionally develop the formation of CNV. If this happens, the presence of neovascular tissue may cause the choroid to seem thicker in some locations. Moreover, patients with GA may present with morphological alteration in the choroid. [115] A decrease in choroidal arteries, especially in the CC layer, which is closely linked to the atrophy areas, could cause choroidal thinning [89]. The choroidal thinning is thought to be associated with reduced perfusion of the RPE and photoreceptors with decreased absorption of oxygen and nutrients playing a role in the degenerative process [126,184]

3.2. nAMD

Patients with nAMD may exhibit different levels of ChT; some may have thicker choroids because of neovascular membranes and related inflammatory processes [97]. On the other hand, some studies have documented progressive choroidal thinning in nAMD, which may be

Table 1
Subfoveal choroidal thickness (SFCT) profile in normal eyes at different ages and in the different types of age-related macular degeneration (AMD).

Authors	Age (years), mean ± SD (range)	Number of eyes	SFCT (μm, range), mean ± SD (range)	Mean AL (mm), mean ± SD (range)
Healthy eyes (ethnicity)				
Chhablani et al. (India) [39]	11.9 ± 3.4	255	312.1 ± 45.40	23.55 ± 0.74
Sanchez-Cano et al. [163]	23.8 ± 3.2	95	345.67 ± 81.80	
Spaide et al. [177]	33.4 (19–54)	17	318 (Right); 335 (Left)	
Rahman et al. (Caucasian, Asian) [147]	38 ± 5	100	332 ± 90	24.46 ± 1.12
Ikuno et al. (Japanese) [83]	39.4 ± 16.0	86	354 ± 111	24.40 ± 1.24
Chhablani et al. (India) [38]	42.8 (21–80)	124	280.1 ± 46.5	22.84 ± 0.78
Ding et al. (Chinese) [51]	49.73 ± 17.89	420	261.93 ± 88.42	
Margolis and Spaide [120]	50.4 (19–85)	54	287 ± 76	
Manjunath et al. [118]	51.1 (22–78)	34	272 ± 81	
Arnould et al. (Caucasian) [8]	81.9 ± 3.6	1494	206.4 ± 83.0	23.37 ± 1.23
dAMD				
Jirarattanasopa et al. [89]	76.3 ± 8.1	64	203 ± 105.9	
Manjunath et al. [119]	78.2 ± 7.9	17	213.4 ± 92.2	
Jonas et al. [90]	77.3 ± 5.8	86	239 ± 84	23.2 ± 0.9
Yiu et al. [207]	74.34 ± 8.32	109	246.0 ± 10.87	
GA				
Lindner et al. [115]	75.97 ± 7.09	72	173.03 ± 90.22	
Sato et al. (Japanese) [165]	76.8 ± 8.8	173	194.7 ± 105.5	23.4 ± 0.9
nAMD				
Manjunath et al. [119]	78.6 ± 7.0	40	194.6 ± 88.4	
Invernizzi et al. [84]	80.5 ± 6.4 (66–93)	65		
-Inactive CNV type 1			178 ± 71	
-Inactive CNV type 2			173 ± 66	
-Active CNV type 1			189 ± 73	
-Active CNV type 2			184 ± 69	
PCV				
Chung et al. [44]	68.5 ± 7.1	25	438.3 ± 87.8	
Jirarattanasopa et al. [89]	73.3 ± 8.0	65	243.3 ± 92.9	
RAP				
Yamakazi et al. [202]	82.2 ± 7.6	19	129.5 ± 35.8	
Kanadani et al. [92]	78.5 ± 5.7	12	182.93 ± 31	
Invernizzi et al. [84]	80.5 ± 6.4 (66–93)	16		
-Inactive RAP			126 ± 43	
-Active RAP			137 ± 50	

SD Standard Deviation, *SFCT* Subfoveal Choroidal Thickness, *AL* Axial Length, *μm* micrometer, *mm* Millimeter, *dAMD* Dry age-related macular degeneration, *GA* Geographic atrophy, *nAMD* Neovascular age-related macular degeneration, *PCV* Polypoidal choroidal vasculopathy, *RAP* Retinal angiomatous proliferation

brought on by atrophic processes or as an adverse effect of photodynamic therapy (PDT) [197].

The nAMD is defined by abnormal new vessel formation from the choroid into the subretinal or sub-RPE region in CNV, resulting in fluid leakage. Because of the underlying CNV in nAMD, an increase in ChT can be seen, particularly in the early neovascular phase. Different choroidal patterns are found in various forms of CNV, including PCV, RAP, and classic CNV [129].

In PCV, which presents with polypoidal vascular lesions in ICGA, the pattern of ChT may be more variable, with isolated thickening areas matching polypoidal lesions [44]. Recent research has indicated that the development of PCV could potentially be due to the dilation of middle and large choroidal vessels that cause choroidal congestion, which subsequently leads to hyperpermeability and an increase in ChT [100].

On the other hand, PDT may have a better effect by inducing vessel remodeling and decreasing ChT; [123] however, it is essential to highlight that there may not be a consistent increase in ChT across the macular area in cases of PCV. Thinning of the choroid may occur in some instances. According to research by Ryu and coworkers,and Baek and coworkers, an ischemia process facilitated by VEGF overexpression might be the primary contributor to PCV in eyes with thin choroids [14,155].

RAP is a pathological condition wherein neovascularization originates from the retina and progresses to the macula. A significant presence of soft drusen or RPD defines it. Although the precise effect of RAP on ChT is not as clear-cut as it is in PCV, ischemic alterations or choroidal insufficiency may cause any underlying choroid thinning [32,92]. Yamazaki and coworkers found that the mean SFCT for 19 cases with RAP was 129.5 ± 35.8 μm, whereas the mean SFCT for 32 age-matched control eyes was 201.3 ± 55.0 μm (p=0.0001). Also, in unilateral RAP, the unaffected fellow eyes showed less mean SFCT compared to the normal eyes ($p = 0.03$). Based on these findings, it appears that patients with unilateral RAP would have already developed choroidal thinning in their fellow eyes, which may not be attributable to the progression or formation of neovascular lesions associated with RAP. There might also be a potential correlation between the choroid and the pathological process of RAP, with the choroidal thinning precipitating reduced oxygen availability in the RPE cells. It has been suggested that the age-related Bruch membrane thickening with lipophilic material disrupts the secretion of VEGF-A from RPE cells toward the CC. Consequently, the absence of VEGF-A may fail to regulate the CC endothelium integrity, resulting in atrophy, as observed histologically in aged eyes. [55,78,148] RAP is more common in older age, often associated with multiple large drusens in affected and unaffected fellow eyes [122], which leads to substantial diffusional disruption of VEGF-A in RAP eyes, potentially inducing CC atrophic changes compared to normal eyes; however, the exact pathophysiological mechanisms remain to be fully understood. [202]. Choroidal circulation abnormalities were also frequently observed in the eyes with RAP lesions and their fellow eyes. On ICGA, decreased choroidal filling was seen in 50 % of fellow eyes of patients with unilateral RAP, in addition to 81.8 percent of eyes with RAP [99]. (Figure 1 and Table 1)

Recently, peripheral choroidal changes have been examined in various diseases. A study by Fukuda and coworkers found that the ratio of posterior ChT (posterior area <9 mm) to peripheral ChT (peripheral area in 9–18 mm) in pachychoroid neovasculopathy (PNV) was significantly higher than in typical AMD ($p < 0.01$); however, there was no significant difference in this ratio between PCV, RAP, and typical AMD. [65] In this study, however, the posterior to peripheral choroidal thickness ratio in RAP was less pronounced than in other subtypes. This may be due to the thickening of the choroid being associated with larger vessels near the vortex vein in the periphery. [65]

3.3. Anti-VEGF treatment

In classic CNV, the ChT beneath the lesion may be increased due to vascular leakage and inflammation [61,205]. Increased vascular flow is observed in the choroid adjacent to CNV regions on OCTA in nAMD patients, and this may be correlated with thicker choroid obtained from structural OCT scans [136]. The ChT may decrease with time and treatment, suggesting either a quiescent phase of the disease or a response to therapy [13]. Repeated intravitreal anti-VEGF injections may induce generalized choroidal thinning, particularly in the CC layer. This

Table 2
Variations in choroidal thickness in physiological conditions and age-related macular degeneration (AMD).

Variations according to different conditions	Choroidal Thickness (ChT)
Physiological variations	
Age	Decreases with age (~13 μm every decade)
Gender	Higher in men
Ethnicity	Slight differences
Axial length (AL)	Decreases with increased AL
Diurnal variations	Thickest at midnight, thinnest at noon
AMD	
dAMD with soft drusen	Decreased
dAMD with reticular pseudodrusen (RPD)	Decreased
dAMD with pachydrusen	Increased
Geographic atrophy (GA)	Decreased
nAMD with exudation	Increased
nAMD inactive	Decreased/equivocal
PCV	Increased
RAP	Decreased

ChT Choroidal thickness, *AL* Axial length, μm Micrometer, *AMD* Age-related macular degeneration, *dAMD* Dry age-related macular degeneration, *RPD* Reticular pseudodrusen, *GA* Geographic atrophy, *nAMD* Neovascular age-related macular degeneration, *PCV* Polypoidal choroidal vasculopathy, *RAP* Retinal angiomatous proliferation

thinning may be indicative of a reduction in neovascularization activity and choroidal vascular hyperpermeability (CVH) [140].

In another study by Yamazaki and colleagues on 40 eyes, including 1 RAP, 16 PCV, and 23 nAMD, they found that ChT decreased significantly during one year of follow-up with a mean of 5.8 injections of intravitreal ranibizumab (baseline: 244±62 μm, after 12 months: 226±66 μm, p=0.002). A notable decrease in ChT was observed in nAMD eyes after 12 months (235±65–218±65; p=0.007)[203]. In contrast, at an 8.4-month mean follow-up, Ellabban and coworkers observed no statistically significant alteration in ChT in 20 eyes with nAMD after ranibizumab injections [53] In various types of nAMD patients, particularly in PNV eyes, a notable reduction in SFCT was observed following 3 monthly intravitreal injections of faricimab. This innovative bispecific monoclonal antibody targets two distinct pathways by simultaneously binding and neutralizing VEGF-A and angiopoietin-2 (Ang-2). This suggests that faricimab may effectively address the underlying choroidal abnormalities associated with pachychoroid phenotypes. [181]

It is crucial to remember that each patient's reaction to anti-VEGF medication is unique and that each patient may experience a different impact on ChT [66]. Therefore, it is imperative to conduct routine monitoring using imaging techniques such as OCT for monitoring purposes to evaluate treatment response and adjust care accordingly [21].

In summary, ChT tends to decrease with age, averaging a reduction of 13μm per decade. The choroid is thicker at midnight and thinner at noon. Men generally have a thicker ChT than women, and slight variations can occur due to ethnicity. Patients with myopia typically have a thinner ChT.

Changes in ChT can serve as biomarkers for different AMD stages, helping distinguish between conditions. In certain circumstances, ChT data can allow for the observation of the natural progression or response to therapy in the course of the disease [121]. For instance, the choroid is thinner in dAMD with soft drusen or RPD, whereas in eyes with pachydrusen, it is thicker. As the eye progresses to GA, complete atrophy of the choriocapillaris occurs, resulting in a thinner choroid. In active nAMD, the choroid thickens, but it thins again when the condition becomes inactive. Eyes with PCV have a thick choroid, while those with RAP show a thin choroid. (Table 2)

4. Choroidal vascularity index

CVI is described as the ratio of the luminal area (LA) to the total choroidal area (TCA) [158 4,27,175] on OCT. To measure CVI, OCT choroidal imaging is conducted, and algorithms are utilized to identify the inner and outer boundaries of the choroidal region. Typically, 1.5 or 3 mm in width, is selected on a line scan for subfoveal CVI measurement, with ImageJ used for image binarization (ImageJ 1.51 s, National Institutes of Health, Bethesda, MD). The 1.5–3 mm width is chosen under the assumption of representing the macular region's segmental blood supply, despite lacking histological basis. Binarization techniques help distinguish stromal and luminal areas, with subsequent calculation of CVI based on the luminal to total choroidal ratio (Figure 2). Branchini and coworkers developed automated software to calculate the dark pixels indicating choroidal stroma, and light pixels indicating vascular lumens.[27] Sonoda and coworkers introduced a technique for calculating luminal and stromal areas using OCT image binarization. [175] Agrawal and coworkers, with modifications to Sonoda and coworkers' technique, proposed the CVI as a measure of choroidal vascular status. They reported that the CVIs in normal eyes range from 65.61 ± 2.33 %, showing less variability compared to ChT. [4] Wide-field CVI assessments in healthy eyes revealed minimal to maximum CVI values across different regions, and the most consistent values are shown in the macular area. The scanning area (subfoveal, central macular, or total macular) does not significantly affect CVI measurement; [2] however, CVI may vary between volume scan and single foveal scan in localized or diffuse choroidal pathologies [172]. In recent studies, CVI has been identified as a significant biomarker in various ophthalmologic conditions, including diabetes mellitus, tubercular multifocal serpiginous choroiditis, Stargardt disease, retinitis pigmentosa, panuveitis, and CSCR [85,173]. Moreover, it has also been widely used in non-ophthalmological diseases including Parkinson disease, Alzheimer disease, multiple sclerosis,

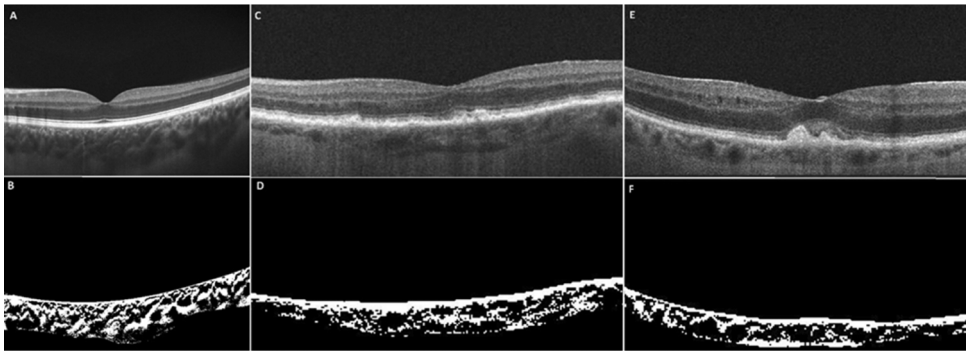

Fig. 2. Choroidal vascular index (CVI) measurement by image binarization of choroidal vessels (the vessels are dark, and the stroma area is bright). The CVI is shown in a 24-year-old healthy eye (Figure 2-A and B), a 65-year-old female which showed soft drusen in optical coherence tomography (OCT), which is in favor of dry age-related macular degeneration (AMD) (Figure 2-C and D), and a 71-year-old male with choroidal neovascularization (CNV), intraretinal and subretinal fluid, in favor of wet AMD (Figure 2-E and F).

idiopathic normal pressure hydrocephalus, and celiac disease. [49,151,182,189,190] A recent study also showed that variable CVI among different ethnicities, where African-American patients were found to have a lower CVI than Caucasians, likely due to a greater proportion of stromal volume. [130] One of the main limitations of this method is that it requires a manual approximation of choroid localization and contrast adjustment, making it less suitable for high-throughput analysis. Addressing this limitation, recent studies introduced a fully automated methodology capable of rapidly and accurately estimating CVI from volume scans and OCT B-scans. Vupparaboina and coworkers demonstrated 40 % improvements in CVI by determining the value of shadow compensation in CVI measurement [194] (Figure 2)

4.1. dAMD and GA

Reduced choroidal vascularity may result in an inadequate supply of nutrients and oxygen to the surrounding retina, making it more vulnerable to the degenerative processes that are typical of AMD [158]. Studies have indicated that AMD may initially be a choroidal vessel pathology, and the CVI evaluation could show additional insights into the vessel structural changes in AMD [29,97,119]. Various imaging modalities can be used to visualize diverse choroidal characteristics associated with different types of drusen and different stages of AMD [198]. Various studies have documented CVI changes, especially in GA or intermediate AMD [198]. Patients diagnosed with AMD had a considerable reduction in CVI, which is connected with clinically significant visual deficits (CVI in AMD, 'normal fellow' eyes and controls were 64.04 ± 2.43 %, 64.66 ± 2.25 %, and 66.07 ± 1.72 %, respectively.) [97]. Wei and coworkers demonstrated a statistically significant difference in CVI between dry and nAMD eyes (60.14 vs. 62.75; p=0.05) [198]. When dAMD progresses, there is frequently a noticeable reduction in CVI, especially in areas where drusen deposition has accumulated. Hard, soft, and cuticular drusen all have different effects on the choroidal vascular architecture, with larger drusen being linked to localized vascular attenuation. Several studies showed how CVI is diminished in cases of GA. Giannaccare and coworkers showed that CVI was reduced in GA (65.83 ± 3.95 vs. 69.33 ± 3.11, $P < 0.001$). [68] Later, Sacconi and coworkers observed a strong association ($r = -0.432$, $P = 0.027$) between the baseline CVI and GA area progression rate. Similarly, they found a substantial correlation ($r = 0.422$, $P = 0.032$) between stromal choroidal area and the rate of GA enlargement, and this reduction frequently correlates with the size and development of atrophic zones [157].

AMD has a much smaller vascular choroidal region compared to normal eyes. Additionally, the CVI varies in impairment across several dAMD cohorts under investigation (drusen, RPD, and GA), indicating a possible role for CVI in characterizing distinct disease cohorts [158]. A cohort study by Sacconi and coworkers on 120 AMD patients found that RPD had lower CVI than controls ($P = 0.040$), and patients with GA had a statistically significant decreased CVI compared to RPD ($P = 0.001$), drusen ($P = 0.046$), and controls ($P < 0.001$) [158].

By decreasing choroidal vessel volume and choroidal blood flow (ChBF), the vessels get smaller and the CVI is expected to decrease. [117] A correlation between elevated drusen extension and reduced ChBF was observed by Berenberg and coworkers [20]. ChB volume (ChB Vol) and ChBF lowered by 0.0061 ($P = 0.03$) and 0.23 ($P = 0.049$) arbitrary units, respectively, for each one-mm^2 increase in the druse area. A substantial inverse relationship was also seen between the average druse area and ChB Vol and ChBF. The ChB and ChBF were reduced by 0.0149 arbitrary units and 0.4951 arbitrary units ($P = 0.001$ and $P = 0.003$, respectively), for each 0.01 mm^2 increase in average druse area [20].

4.2. nAMD

The creation of abnormal blood vessels is a hallmark of nAMD, which is marked by notable alterations in the choroidal vascularity. Different vascular patterns are seen in different CNV subtypes. Wei and coworkers, by conducting a study on 42 unilateral nAMD patients, showed that fellow eyes had significantly higher mean CVI than nAMD eyes (60.14 ± 4.55 vs. 62.75 ± 4.82, $P < 0.01$), but the ChT did not show any significant difference (P=0.93) [198]. Invernizzi and coworkers reported that changes in ChT and CVI may predict nAMD conversion or recurrence before evident clinically. [84]

Variations in CVI may be linked to the occurrence or progression of distinct forms of CNV lesions, even though CVI is not a straightforward tool for classifying the different types of CNV. It is hypothesized that with type 1 CNV, a reduction in CVI could happen because these capillaries could cause the choroid to atrophy with chronicity or displace the normal choroidal vasculature. Since OCT makes it easier to identify subretinal neovascularization in type 2 MNV, the CVI may be more directly affected, especially if the neovascularization causes the underlying choroidal tissue to become disrupted or thickened. Since Type 3 MNV is intraretinal the easiest way to see that is using OCTA and ICGA, which might not have an impact on the CVI; but, as it advances and spreads into the choroidal space, it might have an impact by changing the choroidal structure [3,105]

Two types of PCV including typical PCV (T-PCV) and polypoidal CNV (P-CNV) are reported by Yuzawa and coworkers. The T-PCV shows inner choroidal vessel abnormalities, and the P-CNV exhibits polypoidal-shaped structures at the vessel terminations [210]. A study designed by Batıoğlu and coworkers showed that the T-PCV eyes exhibit significantly higher mean CVI compared to P-CNV eyes ($p = 0.039$), and the intervortex anastomosis diameter was higher in T-PCV than P-CNV [19].

Only one study described the CVI characteristics in patients with RAP. In their study, Kwak and coworkers found that in the unaffected fellow eye of unilateral RAP cases, eyes with lower CVI may be prone to develop CNV. They explained their results considering that choroidal ischemia is caused by reduced choroidal vascularity, which might affect the CNV formation. [103] (Figure 2)

4.3. Anti-VEGF treatment

The clinical significance of CVI in monitoring patients undergoing anti-VEGF injections has still to be elucidated. A previous study by Pellegrini and coworkers described a significant reduction in CVI and ChT after Aflibercept injection for three months in nAMD eyes. [142] These findings were confirmed by following studies that observed a reduction of ChT and CVI after intravitreal anti-VEGF injection treatment in cases with PCV and nAMD. [99,185]

Moreover, Shen and coworkers reported that in CNV, the ChT and CVI increase in response to the overexpression of VEGF, and then return to the pre-exudative status after intravitreal anti-VEGF injections. [169]

5. Choroidal volume

From a clinical standpoint, even with precise estimates of ChT at limited sampling points, evaluating choroidal involvement remains challenging due to CSI irregularity. Therefore, the CVol analysis would be more effective in assessing disease progression and treatment response. Changes in CVol, particularly reductions, may suggest comprehensive choroidal alteration, potentially contributing to the progression of AMD. Methods like enface OCT and EDI-OCT have shown to be quite useful for measuring CVol across different phases of AMD and related disorders.

A study by Barteselli and coworkers revealed that males showed 7.37 % greater CVol compared to females. They also showed that the CVol decreased 0.56 mm^3 (7.59 %) for every millimeter of increasing axial length, and 0.54 mm^3 (7.32 %) per decade [18].

The calculation of CVol entails identifying the CSI at specific regions across multiple scans of OCT. In our prior study, we introduced a manual segmentation technique utilizing EDI-OCT for CVol assessment. Our findings demonstrated minimal variability and an impressive concordance correlation coefficient of 0.99. Additionally, we showed a mean

CVol difference of 0.11 ± 0.12 mm^3 between 2 independent observers [37].

Presently, spectral domain OCT (SD-OCT) or SS-OCT devices do not generate complete 3D volume scans; Instead, they offer uniformly spaced vertical scans. For volume computation, ChT estimates are required at intervening vertical locations. Also, the geometric alignment is compromised by eye movements, which shows further advancement in these devices to enhance to solve these limitations. Consequently, identifying the choroid inner boundary using RPE borders and geometrically aligning all choroid inner boundaries are essential. A method employing probability cones for choroidal vessel segmentation in 3D has been proposed. Initially, multiscale filtering is used to find the surface normal at all voxels, followed by projecting a probability cone at each voxel within a cylindrical region of interest along the surface normal to determine the vessel's core. The presented method utilizes averaged vertical and horizontal raster scans compromising 110 B-scans with a 20-mm separation, to make the volume; Nevertheless, the impact of missing data on vessel segmentation remains unclear. Additionally, this method provides an overall distribution of ChT. [91] The Hessian matrix-based approach is useful for choroidal vessel segmentation by combining choroidal vessel identification and boundary refinement which enhance medical imaging diagnostics and research. [193,211] Comparing different algorithms' accuracy for choroidal quantification and segmentation is challenging due to testing on disparate datasets rather than a standard dataset. Building upon this foundation, we advocated for a rigorous statistical comparison of algorithmic accuracy against 2 pivotal benchmarks: manual reference and observer repeatability. Quotient measures are recommended to make easier comparisons between various methods tested on different datasets. While existing methods primarily focus on vessel segmentation, we have introduced a methodology for quantification and visualization of choroidal vascularity. [193]

Recently, we proposed a common volumetric method for 2D B-scans, for finding the various borders of the choroid layer and Halles sublayer, which makes good smooth spatial continuity. This methodology was done on five normal and five abnormal OCT volumetric scans, considering various metrics including the volumetric Dice coefficient and corresponding quotient measures to facilitate comparison vis-à-vis intra-observer repeatability. The Dice coefficients were 93.53 % for healthy and 93.30 % for diseased OCT volumes, and the reference observer repeatability values for healthy and diseased OCTs were 95.60 % and 95.49 % respectively. [82]

5.1. dAMD and GA

Krytkowska and coworkers evaluated the CVol in 121 healthy controls and 354 AMD cases (175 dAMD and 179 nAMD patients). In comparison to controls and dAMD, they found that nAMD had higher ChT and average volume, and lower CVI [101]. Moreover, they found that choroidal thickness and volume are more affected by hypertension and ischemic heart disease in AMD cases. Early in the dAMD process there may be slight variations in CVol, which frequently match the size and density of drusen. A significant reduction in CVol is indicative of choroidal deterioration as the illness worsens, especially in eyes with significant drusen or those approaching GA. [119].

While the exact mechanisms responsible for alterations in CVol in AMD are not completely known, it is apparent that changes in choroidal circulation, inflammation, and ischemia play a role. Furthermore, it is a result of degeneration in the choroidal vasculature, particularly in the CC, which directly impacts the malfunction of the RPE, production of drusen, and compromised exchange of nutrients and waste. The substantial reduction of CVol in GA signifies a widespread decline in stromal and vascular choroidal elements [22].

5.2. nAMD

On the other hand, nAMD eyes had considerably greater ChT and CVol in the 1-millimeter central ring than did control and dAMD eyes [101]. Furthermore, there were no variations in these characteristics between the healthy eyes and the dAMD eyes. This result is consistent with a study by Noori and coworkers [139], which demonstrated that nAMD eyes had considerably higher mean ChT and CVol of the subfoveal area than dAMD and normal eyes. Similarly, in all subfields of the ETDRS grid, Razavi and coworkers [149] found that nAMD eyes had thicker choroids than healthy control eyes. Edema, exudation, and hemorrhages secondary to active CNV may be the cause of this outcome [101].

The nAMD can cause substantial changes in CVol, typically as a result of the exudation and bleeding that accompany the existence of neovascular membranes. A primary CVol increase may occur because of the creation of neovascular membranes and enhanced vascular permeability. The effects of various MNV subtypes, including PCV, RAP, and classic MNV, on CVol differ [141]. ICGA can confirm the existence of polypoidal lesions in PCV eyes, which frequently show an increased CVol. The polypoidal lesions themselves can be rather noticeable, but the overall CVol alterations may not be as they would be with a conventional CNV [114]. In a research conducted by Vyas and coworkers on 52 eyes belonging to 52 patients with PCV, the CVol of the entire scan region decreased considerably from baseline to month twelve ($p = 0.02$), from 6.7 ± 2.0 mm^3 to 6.3 ± 2.4 mm^3 [195].

Increasing ChT in active neovascularization, according to Invernizzi and coworkers, was not caused by tissue thickening secondary to edema, but rather by choroidal vessel size enlargement with no corresponding increase in vessel density [84]. Increased intraocular VEGF levels may be the cause of this, as it causes choroidal artery dilatation, increased blood flow, and pro-inflammatory and pro-edematous effects [36].

RAP exhibits more drusen, both in area and density, and a smaller subfoveal ChT than typical nAMD. These results may point to a decrease in choroidal perfusion during RAP formation. [94].[94]. The choroid's capacity to provide the RPE and outer retina with an adequate amount of nutrients and oxygen may be compromised by the decreased CVol. [120].

5.3. Anti-VEGF treatment

In general, a localized increase in CVol may occur when the neovascular complex is active. CVol often lowers as the edema and leakage resolve in nAMD patients, especially when treated with anti-VEGF injections. Chronic fluid that is resistant to treatment can result in fibrosis and scarring, which can alter CVol. [208].[208].

The main theories for seeing a drop in CVol following intravitreal anti-VEGF therapy are as follows. Anti-VEGF medications decrease the permeability of the CNVM, reducing the amount of blood and fluid that can seep beneath and inside the retina. As a result, there is a decrease in CVol with reduced choroidal and retinal edema. Moreover, the abnormal blood vessels may shrink in size and number following anti-VEGF therapy, which would reduce CVol. Additionally, it might aid in reducing inflammation inside the choroid, which leads to additional volume reductions. [199].

Patients respond differently to anti-VEGF medication. Some might have a more noticeable reaction, while others might see a significant drop in CVol. The degree of change can vary based on the patient's data, the kind and maturity of the CNV, and the duration of the condition before the initiation of therapy. [199]. Last but not least, when assessing CVol changes, it's critical to take the disease's progress and the efficacy of the treatment into account. For instance, improved visual function is not always translated into a decrease in CVol in cases with irreversible retinal damage.

6. Choroidal vessel layer thickness analysis

Individual choroidal layers may be affected by different diseases, so

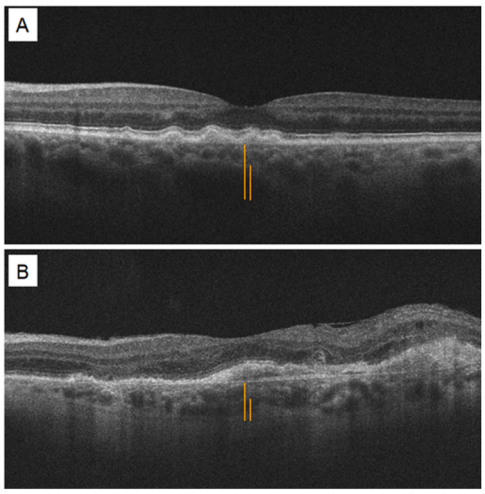

Fig. 3. This figure shows the total choroidal thickness including choriocapillaris (CC), Sattler's and Haller's layers, and the Sattler's layer separately which consists of large choroidal vessels. Figure 3-A**:** In the left eye of a 69-year-old female, the OCT scan shows drusens which are indicators of dry AMD, the total choroidal thickness in the subfoveal area is 252 μm thickness, and the Haller's layer thickness is 162 μm. Figure 3-B**:** This is the left eye of an 83-year-old male with previously active CNV who received multiple intravitreal injections of anti-VEGF, and the CNV became stable. The total choroidal and Haller's layer thickness are decreased (171 μm and 85 μm respectively).

their evaluation may be helpful in clinical practice, as changes are reported in specific layers of the choroid in different diseases; however, delineating a boundary between medium-sized and large-sized vessels proves more difficult than segmenting the outer boundary of the choroid, and even manual segmentation encounters difficulties. The challenge stems from the structural similarities between different choroidal layers and the absence of a clear intensity transition. Consequently, older segmentation methods like gradient-based methods, which are commonly employed for retinal layers, may not be useful. [178] Furthermore, there exists no universally accepted definition for distinguishing between medium-size and large-size vessels. This classification relies solely on the relative vessel diameter but not on predetermined values. Povazay and coworkers have tried to differentiate medium-size and large-size vessels based on vessel density thickness, and cells in the stroma. [143] Recently, a methodology utilizing probability cones on volume scans and an internally developed metric for delineating the boundary of the Haller layer has been introduced. [178] The heuristic approach used to establish the boundary of the Haller layer relies on identifying the largest vessel within a predetermined volume, which could be limiting, particularly in cases where vessels possess larger volumes. Moreover, evaluating the vascular arrangement obtained from the OCT volume scans compared to ICGA may not yield accurate results, and the reported algorithmic precision values compared to manual ones have significant room for enhancement. [187] Additionally, the appropriateness of this approach to single B-scans is unclear. (Figure 3)

To bridge the gap, we explored a method for extracting large-vessel extraction in OCT B-scans. [193] This method builds on our reported binarization technique and employs intuitive statistical criteria. Specifically, it identifies all vessels adjacent to the choroidoscleral interface and categorizes vessels with areas larger than the median value of those detected along the interface as larger vessels. Our evaluation of this method demonstrated high accuracy and a 90 % Dice coefficient compared to a gold standard which is repeatable manual segmentation. Understanding that the distribution of the choroidal vessel layer is often unclear due to its complex nature, we acknowledge that this algorithm may produce spurious results, and manual correction by experts can assist in refining the algorithm's outcomes. [187]

6.1. dAMD and GA

Subtle changes in the CC may be seen in early dAMD, with vessel attenuation or dropout frequently seen in locations beneath drusens. With increasing progression of AMD, these alterations become more noticeable with severe loss of CC, especially in eyes with GA. CC atrophy which is believed to be secondary to RPE destruction and Bruch membrane alterations, is characterized by a lack of CC perfusion [54]. The retinal tissue may become ischemic due to this atrophy, which will accelerate the development of AMD [13]. In addition, the bigger vessels in Haller and Sattler layers may dilate or constrict, which would be consistent with the alterations in the retina [54].

Additionally, choroidal thinning is associated with the loss of choroidal vasculature, possibly due to persistent inflammation and ischemia. Furthermore, abnormalities in the diameter and increased tortuosity of the choroidal vascular system are also observed in dAMD [196].

A study by Lee and coworkers quantified the CC and the Haller vessel characteristics in drusen types of dAMD and pachydrusen compared to control eyes. Using *enface* OCT or OCTA, the diameter, length, and junctions of Haller vessels as well as the overall size, area, and CC flow voids were quantified. While the pachydrusen group's Haller vessel area and diameter were the greatest and its overall length was the shortest, its CC characteristics were comparable to normal eyes. The CC flow void area and size were greatest in the soft drusen within the SDD group, [106].

6.2. nAMD

In a study by Arrigo and coworkers, 1 year of follow-up of dAMD eyes, revealed that Sattler layer thickness was thinner in AMD eyes converting to nAMD compared to eyes that remained dry. Additionally, an increasing CC porosity was seen in OCTA analysis associated with CNV onset. [12] One study by Lee and coworkers showed that the eyes of PCV subjects showed lower CVI ($p = 0.023$), a larger ratio of Haller layer to SFCT ($p < 0.001$), and thicker SFCT ($p < 0.001$) than the eyes of controls. Moreover, in unaffected fellow eyes in comparison to normal eyes, the Haller layer to SFCT ratio was higher ($p<0.001$). [108].

6.3. Anti-VEGF therapy

After intravitreal anti-VEGF injection, the aberrant neovascular networks tend to recede and some of the original choroidal capillaries may potentially regrow. This results in a noticeable alteration in the choroidal vessel layers. On the other hand, long-term anti-VEGF therapy may also affect the natural choroidal circulation, changing the layers of vessels [13].

Anti-VEGF therapies can alter the choroidal vascular layers in several ways by inhibiting VEGF. For instance, anti-VEGF therapies can lessen the growth of new, aberrant vessels in the choroidal layer, which are indicative of CNV linked to nAMD. Moreover, they diminish vessel permeability and fluid reducing leakage, fluid buildup, and retinal edema, which helps to stabilize or improve vision. Also, after anti-VEGF therapy, ChT frequently decreases, as shown by imaging techniques like OCT. The resolution of edema and inflammation in the choroid, along with the regression of CNV, are linked to this reduction in thickness. Another important effect of anti-VEGF therapies is that they normalize the choroidal blood flow, reducing the choroid's aberrant blood flow and determining a retraction of the neovascular network. Anti-VEGF may also lead to a remodeling of choroidal vasculature, resulting in a decrease in both the vessel size and number, especially in the CC. Clinically, these modifications of the choroidal vasculature determine a reduction of hemorrhage and exudates, a normalization of the retinal architecture, and an improvement in visual acuity. On the other hand, long-term anti-VEGF treatment may eventually cause choroidal atrophy or thinning. The RPE and endothelial cells both depend on VEGF for survival, therefore this could be caused by its inhibition [30,180].

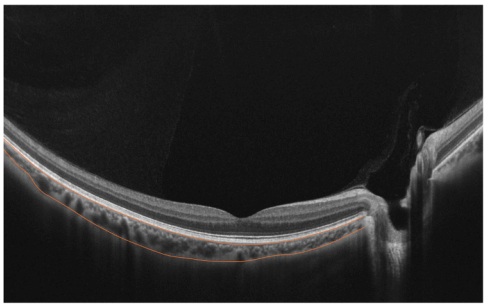

Fig. 4. Choroidal contour in a healthy eye. The upper line shows the Bruch's membrane, and the lower line shows the choroid-sclera interface (CSI).

In conclusion, the capacity to identify and differentiate between the layers of the choroidal vessels, using the imaging techniques discussed above, offers crucial information on the causes, developments, and outcomes of AMD treatments. This multi-layered understanding is necessary for patient care and customized treatment plans.

7. Choroidal contour analysis

The regular choroid is reported to have a bowl-shaped contour, with maximal SFCT which tapers as we go towards the nasal and temporal region. (Figure 4) The arrangement of the choroidal vasculature is continuous, with CC and medium-sized vessels toward the inner aspect and the bigger Haller layer oriented toward the CSI [173]. It has been noted that AMD patients may have focal choroidal thinning, which occurs temporally and gives the appearance of an S-shaped or uneven contour [119]. Legocki and coworkers documented comparable alterations in nAMD patients. Compared to 100 % of normal eyes, 13.3 % of nAMD eyes had a normal bowl-shaped contour. Of the 15 eyes with nAMD, SFCT was the thickest point in 20 % of the eyes compared to 91 % of healthy eyes, and 40 % of patients had focal choroid thinning (vs 0 % of healthy eyes) [109]. When it comes to AMD and its related symptoms, the choroidal contour, which includes the topographic changes and abnormalities in the choroidal layer, has substantial clinical significance [100].

The diverse forms of drusen and the alterations in the cortical shape linked to dAMD are reflections of underlying pathophysiological processes [7]. By evaluating alterations in choroidal thickness, texture, and vasculature, one can distinguish between different types of drusen and phases of dAMD using choroidal contour analysis. These changes may be associated with the severity and progression of the disease. The thinning of the choroid is observed in some patients with dAMD, especially in the latter stages of the disease [60]. As the disease advances to intermediate stages, some patients may start to exhibit choroidal thinning, however, early stages may not show any appreciable choroidal alterations. A few tiny drusen with little effect on choroidal contour may be visible in early AMD. Hard drusen are less frequently linked to significant choroidal alterations than soft and RPD. As dAMD advances, particularly in the direction of GA, the choroid often thins and may exhibit increased heterogeneity in its texture [132].

Changes in the choroidal contour that are predominantly related to the elevations or depressions brought on by underlying drusen may be mild in the early stages of dAMD. With EDI-OCT, these drusen-associated choroidal contour undulations can be seen. The choroidal contour becomes more irregular as dAMD worsens, particularly as it enters the GA phase, and is characterized by thinning areas that match retinal atrophy areas [10].

Because of CNV presence and its impact on the surrounding tissues, choroidal contour examination in nAMD reveals many distinctive changes that are frequently more severe and varied than those seen in dAMD. The formation of neovascular membranes frequently causes significant changes to the choroidal shape in nAMD. With their distinctive polypoidal lesions, the choroidal elevations or protrusions

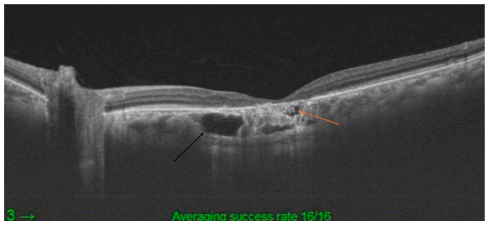

Fig. 5. This figure shows the left eye of an 87-year-old patient with geographic atrophy. The orange arrow shows the type 1 choroidal cavern which is limited to Sattler's layer, and the black arrow shows the type 2 choroidal cavern which is larger than the type 1, in the Sattler's and Haller's layers.

observed in situations such as PCV have a specific choroidal contour that can be clearly recognized on enface OCT and further examined with ICGA. The choroidal contour can also be disrupted to varied degrees by other CNV subtypes, such as RAP and classic CNV, which can be carefully mapped and distinguished utilizing imaging modalities. Following intravitreal anti-VEGF injection, the choroidal contour frequently returns to normal or stabilizes as the neovascular tissue recedes with decreasing edema and exudative alterations. On the other hand, vigorous neovascular activity or long-term therapy may result in persistent abnormalities in shape. Essentially, choroidal contour analysis offers a window into the underlying choroidal processes in AMD, supported by sophisticated ocular imaging. It is critical to comprehend these contours to evaluate the severity of the disease, measure the effectiveness of treatment, and forecast the course of the illness [26].

In a recent retrospective study we included 13 healthy eyes, 12 eyes with CSCR, and 8 eyes with AMD. A widefield SS-OCT was used to acquire volumetric images, and the previously proven residual U-net (ResUnet) deep learning model for choroidal segmentation was used to produce a choroidal inner surface and outer surface in three dimensions. Using a specially designed 3D visualization tool based on MATLAB, a qualitative analysis of the choroidal inner surface and the choroidal outer surface was carried out, and the choroidal contour shapes were arranged in decreasing steepness order. The maximum primary curvature (Pmax) of the surface, which was determined at the superior, inferior, temporal, and nasal macula, served as the basis for the quantitative analysis. In conclusion, compared to normal eyes, the choroidal contour was flatter in AMD [10].

In a separate cross-sectional investigation, 15 eyes with nAMD and 11 normal eyes were evaluated by single horizontal high-definition raster line imaging employing high-definition SD-OCT. Under the fovea, two separate graders evaluated the choroidal anatomy and quantified the vascular layer thickness. In eyes with nAMD compared to healthy eyes, significant thinning was seen in the CC and medium choroidal vessel layer (205.7 μm ± 17.08 μm versus 281.3 μm ± 19.29 μm, P =0.007), the large choroidal vessel layer (174.1 μm ± 16.34 μm versus 244.5 μm ± 19.51 μm, P =0.01), and the SFCT (31.53 μm ± 3.67 μm versus 51.9 μm ± 1.94 μm, P =0.0002). Finally, as determined by SD-OCT, choroidal morphology is changed in eyes suffering from nAMD. In nAMD, all the vascular layers are involved in choroidal thinning. These anatomical and vascular alterations could have therapeutic ramifications for identifying and tracking nAMD in the eyes [109].

Most investigations use line scans, which yield 2D features of the choroidal contour [109]. To investigate localized differences in choroidal contour, choroidal thickness maps provide more comprehensive and reliable information.

The choroidal contour can show how AMD is progressing; a thin choroid may indicate a greater chance of atrophic alterations. It is possible to forecast the likelihood of progression to GA or nAMD, based on the location and pattern of choroidal alterations. The link between the choroid and retinal alterations in AMD can be better understood with the use of choroidal contour analysis. Making treatment decisions, keeping an eye on the course of the disease, and getting an early

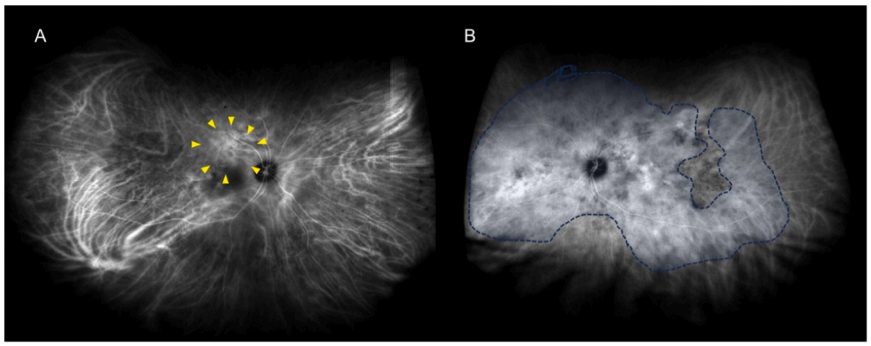

Fig. 6. Differences in choroidal vascular hyperpermeability between eyes with PNV Late phase ICGA (of 10 min after dye injection) shows a focal area of choroidal vascular hyperpermeability (CVH) in A and diffuse CVH in B. This difference may be caused by a difference in severity of vascular change or pathophysiology.

diagnosis all depend on this.

8. Choroidal caverns

In a previous study by Querques and coworkers the incidence of "choroidal caverns" was documented in 12.5 % of eyes affected by GA. These caverns are described within the Sattler layer of the choroid, localized in regions devoid of choroidal vessels. (Figure 5) The etiology of these caverns is postulated to involve the absence of flow signal ghost vessels and the persistence of stromal pillars. [52,145]. The choroidal caverns are classified into 2 types by Guo and coworkers. Type 1, which is small and lobulated in choriocapillaris and Sattler's layer and is seen in 17.4 % of normal eyes and 1.6 % of nAMD, and type 2 which is seen in Sattler and Haller layers, has a larger diameter, and it is present in 0 % of normal eyes, and 21.3 % of nAMD. They showed that the number, thickness, and width of type 2 choroidal caverns demonstrate associations with macular ChT, and this type is more seen in RPE atrophic retinal diseases. [72]

It is not only seen in AMD but also in various retinal diseases and healthy eyes, and it could be physiologically choroidal lipid material, from the photoreceptor metabolism. [52,162] It is not associated with other OCT findings in GA including general thinning, outer retina tubulation, retinal pseudocyst, ghost drusen, and wedge-shaped hyporeflective lesions between Bruch membrane and outer plexiform layer. [145]

9. Choroidal vascular hyperpermeability

CVH contributes to the CSCR, PCV, and nAMD [41,89]. CVH results in elevated hydrostatic pressure, which causes an increased ChT, micro-RPE separation, and RPE tears in eyes with PCV. CVH is most effectively diagnosed during the late phase of ICGA with multifocal choroidal hyperfluorescence [89,138]. It is related to choroidal anatomical parameters including ChT and CVD, and previous research showed that the eyes with CVH had higher SFCT. (Figure 6)

There are differences in CVH in eyes with or without pachychoroid phenomenon, between macular CNV subtypes. Eyes with CNV related to PCV showed more CVH incidence than AMD. [15,164] Recent studies showed a relatively worse response to intravitreal anti-VEGF injections in eyes with higher ChT and CVH. The treatment response differs between groups with and without CVH in PCV patients. Patients with thick choroids and CVH as determined by ICGA had a poor response to intravitreal anti-VEGF injection therapy and a less favorable visual outcome [75,98,155,171,204].

10. Choroidal vascular density

The morphology of choroidal vessels may be an important feature for choroidal evaluation in AMD. The choroidal vascular density (CVD) is a quantification report of vascularity status which is measured by OCTA at 100 μm beneath Bruch membrane. (142) It has been shown that it is affected by the aging process too. Ruiz-Medrano and coworkers reported that the healthy subjects older than 18 years had significantly lower CVD than younger subjects. [154] Fujiwara and coworkers reported that in healthy eyes, CVD is affected by age and SFCT. [64]

Alten and coworkers by evaluating 186 eyes with SDD showed that the CVD from enface slabs is significantly lower in eyes with SDD (143), but with a similar approach, another report from Laíns and coworkers did not show any significant differences in CVD in eyes with SDDs. (144) On en face OCT of the Haller layer, there was a significant difference in the morphology of vessel pattern between PCV and AMD. [15] Lee and coworkers demonstrated higher CVD in PCV and PNV eyes compared to AMD using ultra-widefield ICGA. [104]

PNV and PCV are characterized by a thickened choroid and intervortex venous anastomoses. These observations suggest that the abnormal dilation of deep choroidal vessels, including those in the peripheral regions, may play a significant role in the pathophysiology of PNV and PCV. [125] Ra and coworkers reported that in PCV eyes, the CVD was significantly higher compared to the healthy control group in most regions including the periphery. Moreover, there was a positive correlation between CVD and ChT also the CVH, suggesting that choroidal congestion and dilatation play an important role in PCV pathogenesis. Additionally, the higher CVD and ChT were correlated with poor response to intravitreal anti-VEGF injections. [146]

11. OCTA of the choroid

En face imaging with OCTA enables the observation of the choroidal vasculature in vivo. This imaging entails capturing multiple OCT scans at consistent locations and analyzing the motion contrast to understand blood flow characteristics. [67,116]

Over the last decade, technological advancements have significantly transformed medical imaging. Innovations have emerged, leveraging either doppler shift or decorrelation principles. [79,80,86,168] Notably, the split-spectrum amplitude-decorrelation angiography (SSADA) algorithm, pioneered by Huang and collaborators, has played a pivotal role. This algorithm enhances image acquisition by increasing the number of frames captured, leading to improved signal-to-noise ratios; however, it comes at the cost of diminished axial resolution. [86]

Another notable adaptation in this field is optical microangiography, which cleverly combines both amplitude-based and phase-based approaches, allowing for comprehensive and detailed visualization of microvascular structures. [67] In normal eyes, CC in OCTA is characterized by alternating patterns of dark areas, representing voids signal, and bright areas, representing blood flow. [42]. Signal voids may occur either from areas of flow void due to decreased contrast concentration or from regions with blood flow below the detectable threshold. It has been shown that signal void areas due to the loss of contrast concentration tend to increase with age. [25] The highest density of capillaries is found at

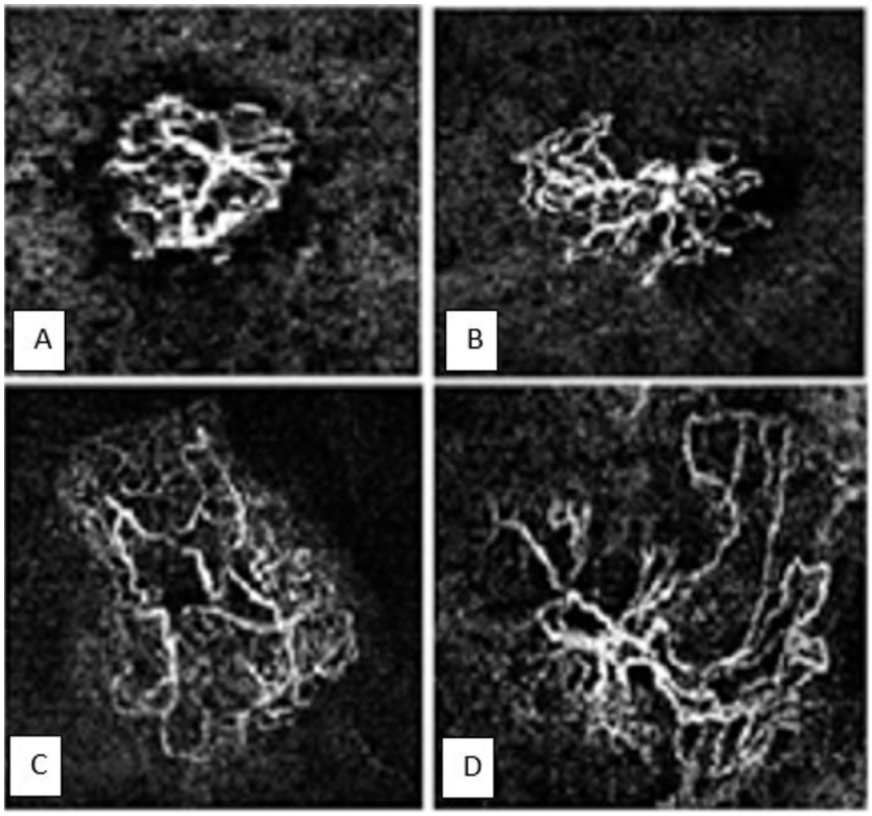

Fig. 7. Various choroidal neovascularization (CNV) patterns in optical coherence tomography angiography (OCTA). Figure 7-A**:** a central feeder vessel with Medusa pattern. Figure 7-B**:** eccentric feeder vessel with Seafan pattern. Figure 7-C**:** No feeder vessel and Indistinct pattern. Figure 7-D**:** A main vascular trunk without thin branches called Pruned vascular tree. [179] **Note:** Permission to use this figure has been obtained from the Indian Journal of Clinical and Experimental Ophthalmology editorial board.

the fovea and diminishes progressively with distance from it. Nowadays, OCTA has become essential in managing patients with AMD, as it can evaluate choroidal circulation flow, vessel density, and qualitatively and quantitatively assess CNV in AMD.

Compared to using multiple instruments for multimodal imaging, a single SS-OCTA scan offers a convenient, comfortable, and comprehensive method for obtaining both qualitative and quantitative anatomic and angiographic information. This approach effectively monitors the onset, progression, and response to therapies in both nonexudative and exudative AMD. [153]

11.1. Dry AMD and GA

In cases of dAMD, a single SS-OCTA scan was utilized to detect and measure various structural features in the macula. These features included the area and volume of typical soft drusen and calcified drusen, the presence and location of hyperreflective foci, the presence of RPD, the thickness of the outer retinal layer, the presence and thickness of basal laminar deposits, the presence and area of persistent choroidal hypertransmission defects, and the presence of treatment-naïve nonexudative macular neovascularization. [153]

The dAMD eyes have shown decreased CC density in OCTA scans. [24,43,87] In cases of intermediate AMD, the regions of CC reduction were primarily observed beneath and near the area of drusen. [24] A similar decrease in CC blood flow has been documented in eyes exhibiting RPD, and the decline in CC vessel density was observed to align with the quantity of RPD lesions. [6]

Research by Li and coworkers, however, revealed that eyes affected by macular RPD exhibited reduced macular CC perfusion, decreased CC thickness, and diminished macular ChT measurements compared to healthy eyes or eyes with soft drusen. Hence, the emergence of RPD in AMD might be attributed to a deficiency in choroidal perfusion, as supported by findings from other comparable research groups. [1,110] Nam and coworkers showed varying patterns of decreased vessel perfusion in all slabs for intermediate AMD with RPD versus intermediate AMD without eyes. [134]

Conversely, Wu and coworkers found no significant discrepancies in CC flow void and average ChT, indicating that RPD did not affect vascular parameters in an intermediate stage of dry AMD. [200]

Alterations in CC vascular density could offer insights into the AMD progression, transitioning from early stages to advanced stages like GA. [45,46] A recent study by Nattagh and coworkers showed that there was a significant correlation between the expansion rate of GA and the density of CC flow void in both the macular area and the region surrounding the margin of GA. The level of flow void surrounding GA was linked to the growth of GA into that specific region. Moreover, Greig and coworkers showed that a significant decrease in CC blood flow may be seen locally before the GA development. [135]

Where drusen and RPE alterations are present, OCTA can identify reduced CC layer density and flow [96]. The "honeycomb" type of CC pathology was observed beside large drusen, with normal interval areas in between, while a normal CC feature, disrupted by small black holes, indicated the presence of drusen. It has been observed that the nearly complete absence of CC perfusion is primarily seen in the large, closely spaced drusen. Additionally, CC non-perfusion may extend beyond well-defined drusen. This could be explained by the impact on nutritional needs in the vicinity of large drusen associated with dAMD. [33,70]

11.2. nAMD

In eyes with nAMD, the same SS-OCTA scan pattern was utilized to detect and measure macular fluid, identify the presence and type of

CNV, and assess the exudation response to anti-VEGF treatment. This scan pattern was also used to quantify CC perfusion, CC thickness, choroidal thickness, and choroidal vascularity. [153]

The emergence of nAMD typically manifests with intraretinal and subretinal fluid detected in the OCT scans; however, a particular subgroup referred to as non-exudative CNV (neCNV) comprises treatment-naive MNV without exudative features ("inactive" CNV) observed on OCT B-scans for a minimum of six months. [144]

OCTA is becoming the favored diagnostic instrument for identifying these lesions. During the initial 12 months, the likelihood of progressing to exudation is significantly greater in eyes with neCNV than in those with dAMD (21.1 % vs. 3.6 %). [50] Various groups have attempted to pinpoint neCNV growth and exudation predictors using OCTA; however, the effectiveness of OCTA biomarkers as precise predictors of CNV activity is unrecognized. [186] Even though neCNV has usually been identified in the aspect of intermediate dAMD, it has also been associated with GA. [31] In these cases, treatment should be reserved only for exudation, secondary to the protective effect of neCNV on GA progression delay. [73,156] Additionally, OCTA enhances the examination of exudative CNV since alternative techniques like FA and ICGA offer lower resolution and are prone to dye leakage. [133]

High vessel tortuosity in CNV observed through OCTA may negatively correlate with deep capillary plexus vessel density and visual outcomes. Additionally, it is significantly associated with a higher onset of retinal atrophy. [11] Previous studies showed that in type 1 CNV, the OCTA shows special features of new vessels such as medusa head, sea fan, or tangled patterns, while in type 2 CNV, it shows a main trunk with sharp demarcation and dense smaller vessel branching networks. [48,102] (Figure 7)

In addition to morphological characteristics, various quantitative parameters such as CNV area, vessel density, and flow index have been identified. Jia and coworkers observed a choroidal blood flow decrease in five neovascular AMD patients, with CNVM areas ranging from 0.13 to 2.18 mm^2 and CNV flow index values ranging from 0.120 to 0.148. The flow index, which is a ratio derived from vessel density and velocity within the CNVM complex, demonstrated higher values in eyes with large CNV, type 2 CNV, or combined CNV. [88]

Remarkably, PCV exhibits diverse OCTA patterns. This neovascular lesion manifests as a polyp (nodular vascular agglomeration) alongside a branching vascular network situated beneath sub-RPE. [35] Despite OCTA's variable sensitivity and specificity in detecting PCV, ICGA remains the gold standard for diagnosis. While the branching vascular network detection via OCTA is comparable to or even surpasses ICGA, the presence of an aneurysmal lesion might elude OCTA when slow flow fills the polyp. [58]

Furthermore, OCTA has significantly expanded our comprehension of the pathophysiology involved in type 3 CNV. This technology unequivocally revealed the intraretinal origin of these lesions from the deep vascular complex and the subsequent events leading to their development. [161]Moreover, OCTA has corroborated the role of CC ischemia in the formation of type 3 CNV in both the diseased eyes and fellow eyes. [159,160]

11.3. Anti-VEGF response

OCTA plays a crucial role in the treatment decision-making process for nAMD, to identify the type of CNV, assess disease activity, and evaluate the usefulness of intravitreal anti-VEGF injection therapy. With a demonstrated sensitivity of 50 % and specificity of 91 % in the diagnosis of CNV secondary to nAMD, OCTA is an invaluable instrument for disease assessment [69]. Previous studies showed that after treating nAMD, the size of the CNV and the density of the neovascularization complex decreased, accompanied by morphological alterations in the CNV. Moreover, the morphology of CNV varied between active and quiescent forms, notably, active CNV lesions exhibited more small branching vessels and peripheral arcades compared to quiescent CNV. [5,47,128]

Kim and coworkers showed that the site of neovascularization in nAMD in OCTA of their 53 patients differed in the responses to anti-VEGF treatment. Following anti-VEGF treatment, type 2 neovascularization considerably reversed in comparison to type 1 neovascularization [95].

The angiographic patterns of CNV have also been summarized as immature (tangle CNV), mature (medusa, and sea-fan CNV), and hyper mature (dead-tree CNV). Immature forms were characterized by a higher risk of growth, whereas mature and hypermature features showed a moderate progression and a resistance to injection therapy. [17,201]

Apart from the baseline analysis, quantitative OCTA-based changes have been described in the treated eyes with CNV. Kuehlewein and coworkers calculated the area of type 2 CNVM in the n-AMD eyes. After treatment with ranibizumab at 2 months, there was a size reduction (4.12–1.64 mm^2) and vessel density of 19.83–7.57 mm^1; however, the main vascular trunk remains unchanged in size. Muakkassa and coworkers measured the area and greatest linear dimension of CNVM on OCTA in multiple chorioretinal diseases (nAMD, PCV, CSCR-related CNVM, multifocal choroiditis, and MacTel-related neovascular membrane) in 6 eyes. After anti-VEGF injections, there was an average reduction in the greatest linear dimension (23.6 %) and area of CNVM (29.8 %) in 5 eyes. [102,131].

12. Conclusions

Age-related macular degeneration encompasses a range of diseases with diverse risk factors resulting in various subtypes. Advancements in retinal optical imaging techniques, such as enhanced depth imaging OCT and OCTA, have enhanced our comprehension of the choroid and provided high-resolution images of the retina and choroid and their vasculature. These techniques are noninvasive and easily reproducible, making them indispensable in diagnosing and assessing treatment outcomes for macular and retinovascular diseases; however, the limited choroidal penetration of OCT devices hinders the resolution of images. Furthermore, the sensitivity and specificity of these choroidal parameters in diagnosing diseases can still be improved. Various biomarkers have been identified and analyzed in AMD, leading to the possibility of personalized treatment. Acquiring more accurate quantification on choroidal biomarkers, including ChT, CVol, CVI, CVH, CVD, choroidal vascular layer thickness, choroidal contour, and choroidal caverns, in addition to EDI-OCT, OCTA, and enface images, would enhance our knowledge of AMD.

Variations in ChT are seen in different stages of AMD, with thinning or increased thickness depending on the stage and the drusen type. In nAMD, the ChT varies due to active or inactive CNV or receiving anti-VEGF injection. Reduced CVI in AMD, especially in GA, is linked to visual deficits and disease progression. Reduced CVol indicates choroidal deterioration in AMD, especially in GA, but nAMD may show increased CVol initially and decrease by anti-VEGF therapy. Subtle changes in CC are seen in early-stage AMD and become more noticeable as the disease progresses. Anti-VEGF therapy reduces abnormal neovascular networks and fluid leakage, normalizes blood flow, and remodels vasculature, but long-term use may lead to choroidal atrophy or thinning. AMD patients often exhibit choroidal thinning, leading to an uneven contour, which can be analyzed using EDI-OCT to distinguish between different types of drusen and phases of AMD. Anti-VEGF therapy can normalize or stabilize the choroidal contour in nAMD, which shows significant changes due to neovascular membranes, with more severe and varied alterations than dAMD. Choroidal caverns and CVH are associated with different stages of AMD. CVD is higher in PCV and PNV eyes compared to AMD, suggesting that choroidal congestion and dilatation play a significant role in PCV pathogenesis and are correlated with poor response to anti-VEGF injections. OCTA is essential for evaluating choroidal circulation, vessel density, and CNV in AMD, with SS-OCTA providing

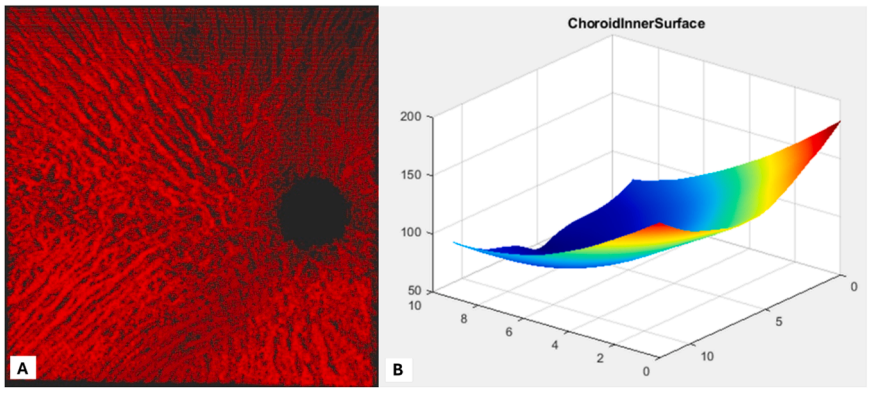

Fig. 8. Future directions of choroidal analysis. Figure 8-A**:** This figure shows the 3-dimensional (3D) view of choroidal vessels. Figure 8-B**:** This figure shows the 3D choroidal contour analysis.

comprehensive information to monitor disease progression and therapy response. Studies on peripheral choroidal changes in AMD are limited and need more consideration. These choroidal biomarkers require further validation to be introduced into clinical practice, providing insight into innovative diagnostic and therapeutic interventions for choroidal diseases.

13. Future directions

Current imaging techniques for evaluating choroid have provided valuable findings in choroidal changes of AMD; however, a comprehensive visualization of the choroid with deeper penetration and higher resolution is needed for better analysis of choroidal structures (vessels and stroma) and choroidal parameters such as thickness and contour. At present, modalities often provide qualitative findings in choroidal changes such as CVH in ICG images, whereas quantification of parameters may help researchers to identify changes in patient visits. 3D evaluation of choroidal vessels, measurements, and segmentation can aid in better identification of different parameters that are not represented in a single 2D scan. Choroidal contour is a fairly newer entity that has attracted researchers, and the advent of 3D maps of choroidal vessels and contour analysis has opened up new dimensions and possibilities previously unexplored.[9,81] (Figure 8)

In summary, the collaborations between ophthalmologists and engineers, by using artificial intelligence will drive the development of new algorithms to make high resolution 3-dimensional scans to enhance our knowledge about AMD, and better assessment of choroidal biomarkers, to improve patient care.

Method of literature

This review article delves into the latest developments in choroidal analysis for age-related macular degeneration (AMD). Our methodology primarily relies on meticulously curated English-language publications spanning the past two decades, with a keen focus on the most recent five years. We meticulously scoured databases such as PubMed and Google Scholar to identify relevant studies.

Funding

We confirm that no funding was received for the execution of this manuscript.

CRediT authorship contribution statement

Mohammed Nasar Ibrahim: Writing – review & editing. **Kiran Kumar Vupparaboina:** Writing – review & editing. **Jiwon Baek:** Writing – review & editing. **Mohammed Abdul Rasheed:** Writing – review & editing. **Elham Rahmanipour:** Writing – original draft. **Nicola Valsecchi:** Writing – review & editing, Writing – original draft. **Nasiq Hasan:** Writing – review & editing. **Mahsa Ejlalidiz:** Writing – original draft. **Elham Sadeghi:** Writing – review & editing, Writing – original draft, Supervision, Resources, Project administration, Methodology, Investigation. **Jay Chhablani:** Writing – review & editing, Supervision, Project administration, Methodology, Conceptualization. **Danilo Iannetta:** Writing – review & editing.

Declaration of Competing Interest

We wish to confirm that there are no known conflicts of interest associated with this publication and there has been no significant financial support for this work that could have influenced its outcome. We confirm that the manuscript has been read and approved by all named authors and that there are no other people who satisfied the criteria for authorship but are not listed. We further confirm that the order of authors listed in the manuscript has been approved by all of us. We further confirm that any aspect of the work covered in this manuscript that has involved has been conducted with the ethical approval of all relevant. We understand that the Corresponding Author (Jay Chhablani MD) is the sole contact for the Editorial process (including Editorial Manager and direct communications with the office). He is responsible for communicating with the other authors about progress, submissions of revisions and final approval of proofs. We confirm that we have provided a current, correct email address which is accessible by the Corresponding Author.

References

1. Abdolrahimzadeh S, Zweifel SA, Di Pippo M, et al. Central macular choriocapillaris impairment as a manifestation of microvascular disease in eyes with subretinal drusenoid deposits. *Eye*. 2024;38:173–178.
2. Agrawal R, Wei X, Goud A, et al. Influence of scanning area on choroidal vascularity index measurement using optical coherence tomography. *Acta Ophthalmol*. 2017;95:e770–e775.
3. Agrawal R, Ding J, Sen P, et al. Exploring choroidal angioarchitecture in health and disease using choroidal vascularity index. *Prog Retin Eye Res*. 2020;77, 100829.
4. Agrawal R, Gupta P, Tan K-A, et al. Choroidal vascularity index as a measure of vascular status of the choroid: measurements in healthy eyes from a population-based study. *Sci Rep*. 2016;6:21090.
5. Al-Sheikh M, Iafe NA, Phasukkijwatana N, Sadda SR, Sarraf D. Biomarkers of neovascular activity in age-related macular degeneration using optical coherence tomography angiography. *Retina*. 2018;38:220–230.
6. Alten F, Heiduschka P, Clemens CR, Eter N. Exploring choriocapillaris under reticular pseudodrusen using OCT-Angiography. *Graefes Arch Clin Exp Ophthalmol*. 2016;254:2165–2173.
7. Amato A, Arrigo A, Borghesan F, et al. Baseline sattler layer–choriocapillaris complex thickness cutoffs associated with age-related macular degeneration progression. *Retina*. 2022.
8. Arnould L, Seydou A, Gabrielle P-H, et al. Subfoveal choroidal thickness, cardiovascular history, and risk factors in the elderly: the Montrachet study. *Invest Ophthalmol Vis Sci*. 2019;60:2431–2437.

9. Arora S, Singh SR, Rosario B, et al. Three-dimensional choroidal contour mapping in healthy population. *Sci Rep*. 2024;14:6210.
10. Arora S, Rosario B, Selvam A, et al. Three-dimensional choroidal contour mapping in pathology: comparison with healthy controls. *Invest Ophthalmol Vis Sci*. 2022;63:483-A0020.
11. Arrigo A, Saladino A, Aragona E, et al. Clinical and imaging biomarkers associated with outer retinal atrophy onset in exudative age-related macular degeneration: a real-word prospective study. *Ophthalmol Ther*. 2024;13:1185–1196.
12. Arrigo A, Amato A, Barresi C, et al. Choroidal modifications preceding the onset of macular neovascularization in age-related macular degeneration. *Ophthalmol Ther*. 2022;11:377–386.
13. Arya M, Sabrosa AS, Duker JS, Waheed NK. Choriocapillaris Changes in Dry Age-Related Macular Degeneration and Geographic Atrophy: A Review. *Eye Vis*. 2018.
14. Baek J, Lee JH, Lee WK. Clinical relevance of aqueous vascular endothelial growth factor levels in polypoidal choroidal vasculopathy. *Retina*. 2017;37:943–950.
15. Baek J, Lee JH, Jung BJ, Kook L, Lee WK. Morphologic features of large choroidal vessel layer: age-related macular degeneration, polypoidal choroidal vasculopathy, and central serous chorioretinopathy. *Graefe'S Arch Clin Exp Ophthalmol*. 2018;256:2309–2317.
16. Bakri SJ, Thorne JE, Ho AC, et al. Safety and efficacy of anti-vascular endothelial growth factor therapies for neovascular age-related macular degeneration: a report by the American Academy of Ophthalmology. Ophthalmology. 2019;126:55–63.
17. Barayev E, Meshi A, Gershoni A, et al. Optical coherence tomography angiography patterns of type 1 macular neovascularization in age-related macular degeneration patients, 11206721221150535 *Eur J Ophthalmol*. 2023.
18. Barteselli G, Chhablani J, El-Emam S, et al. Choroidal volume variations with age, axial length, and sex in healthy subjects: a three-dimensional analysis. *Ophthalmology*. 2012;119:2572–2578.
19. Batıoğlu F, Yanık Ö, Özer F, Demirel S, Özmert E. A comparative study of choroidal vascular and structural characteristics of typical polypoidal choroidal vasculopathy and polypoidal choroidal neovascularization: OCTA-based evaluation of intervortex venous anastomosis. *Diagnostics*. 2022;13:138.
20. Berenberg TL, Metelitsina TI, Madow B, et al. The association between drusen extent and foveolar choroidal blood flow in age-related macular degeneration. *Retina*. 2012;32:25–31.
21. Bezerra HG, Costa MA, Guagliumi G, Rollins AM, Simon DI. Intracoronary optical coh erence tomography: a comprehensive review. *Jacc Cardiovasc Interv*. 2009.
22. Bhutto IA, McLeod DS, Jing T, et al. Increased choroidal mast cells and their degranulation in age-related macular degeneration. *Br J Ophthalmol*. 2016.
23. Bhutto IA, Baba T, Merges C, McLeod DS, Lutty GA. Low nitric oxide synthases (NOSs) in eyes with age-related macular degeneration (AMD). *Exp eye Res*. 2010;90:155–167.
24. Borrelli E, Shi Y, Uji A, et al. Topographic analysis of the choriocapillaris in intermediate age-related macular degeneration. *Am J Ophthalmol*. 2018;196:34–43.
25. Borrelli E, Sarraf D, Freund KB, Sadda SR. OCT angiography and evaluation of the choroid and choroidal vascular disorders. *Prog Retin Eye Res*. 2018;67:30–55.
26. Branchini L, Regatieri C, Adhi M, et al. EFfect of intravitreous anti–vascular endothelial growth factor therapy on choroidal thickness in neovascular age-related macular degeneration using spectral-domain optical coherence tomography. *JAMA Ophthalmol*. 2013;131:693–694.
27. Branchini LA, Adhi M, Regatieri CV, et al. Analysis of choroidal morphologic features and vasculature in healthy eyes using spectral-domain optical coherence tomography. *Ophthalmology*. 2013;120:1901–1908.
28. Breher K, Terry L, Bower TGR, Wahl S. Choroidal biomarkers: a repeatability and topographical comparison of choroidal thickness and choroidal vascularity index in healthy eyes. *Transl Vis Sci Technol*. 2020.
29. Cabrera A, Stoddard J, Tierno IS, et al. Increased cell stiffness contributes to complement-mediated injury of choroidal endothelial cells in a monkey model of early age-related macular degeneration. *J Pathol*. 2022.
30. Calzetti G, Mora P, Borrelli E, et al. Short-term changes in retinal and choroidal relative flow volume after anti-vegf treatment for neovascular age-related macular degeneration. *Sci Rep*. 2021.
31. Capuano V, Miere A, Querques L, et al. Treatment-naïve quiescent choroidal neovascularization in geographic atrophy secondary to nonexudative age-related macular degeneration. *Am J Ophthalmol*. 2017;182:45–55.
32. Cebeci Z, Kır N. All types of age-related macular degeneration in one patient. *Turk J Ophthalmol*. 2017.
33. Chatziralli I, Theodossiadis G, Panagiotidis D, Pousoulidi P, Theodossiadis P. Choriocapillaris vascular density changes in patients with drusen: cross-sectional study based on optical coherence tomography angiography findings. *Ophthalmol Ther*. 2018;7:101–107.
34. Cheung CMG, Gan A, Yanagi Y, Wong TY, Spaide R. Association between choroidal thickness and drusen subtypes in age-related macular degeneration. *Ophthalmol Retin*. 2018;2:1196–1205.
35. Cheung CMG, Lai TY, Ruamviboonsuk P, et al. Polypoidal choroidal vasculopathy: definition, pathogenesis, diagnosis, and management. *Ophthalmology*. 2018;125:708–724.
36. Chhablani J, Barteselli G. Clinical applications of choroidal imaging technologies. *Indian J Ophthalmol*. 2015;63:384–390.
37. Chhablani J, Barteselli G, Wang H, et al. Repeatability and reproducibility of manual choroidal volume measurements using enhanced depth imaging optical coherence tomography. *Invest Ophthalmol Vis Sci*. 2012;53:2274–2280.
38. Chhablani J, Rao PS, Venkata A, et al. Choroidal thickness profile in healthy Indian subjects. *Indian J Ophthalmol*. 2014;62:1060.
39. Chhablani JK, Deshpande R, Sachdeva V, et al. Choroidal thickness profile in healthy Indian children. *Indian J Ophthalmol*. 2015;63:474.
40. Chirco KR, Sohn EH, Stone EM, Tucker BA, Mullins RF. Structural and molecular changes in the aging choroid: implications for age-related macular degeneration. *Eye*. 2017;31:10–25.
41. Cho HJ, Kim HS, Jang YS, et al. Effects of choroidal vascular hyperpermeability on anti–vascular endothelial growth factor treatment for polypoidal choroidal vasculopathy. e1191 *Am J Ophthalmol*. 2013;156:1192–1200.
42. Choi W, Mohler KJ, Potsaid B, et al. Choriocapillaris and choroidal microvasculature imaging with ultrahigh speed OCT angiography. *PLoS One*. 2013;8, e81499.
43. Choi W, Moult EM, Waheed NK, et al. Ultrahigh-speed, swept-source optical coherence tomography angiography in nonexudative age-related macular degeneration with geographic atrophy. *Ophthalmology*. 2015;122:2532–2544.
44. Chung SE, Kang SW, Lee JH, Kim YT. Choroidal thickness in polypoidal choroidal vasculopathy and exudative age-related macular degeneration. *Ophthalmology*. 2011;118:840–845.
45. Corvi F, Tiosano L, Corradetti G, et al. Choriocapillaris flow deficits as a risk factor for progression of age-related macular degeneration. *Retina*. 2021;41:686–693.
46. Corvi F, Corradetti G, Tiosano L, et al. Topography of choriocapillaris flow deficit predicts development of neovascularization or atrophy in age-related macular degeneration. *Graefes Arch Clin Exp Ophthalmol*. 2021;259:2887–2895.
47. Coscas F, Lupidi M, Boulet JF, et al. Optical coherence tomography angiography in exudative age-related macular degeneration: a predictive model for treatment decisions. *Br J Ophthalmol*. 2018.
48. Dansingani KK, Freund KB. Optical coherence tomography angiography reveals mature, tangled vascular networks in eyes with neovascular age-related macular degeneration showing resistance to geographic atrophy. *Ophthalmic Surg, Lasers Imaging Retin*. 2015;46:907–912.
49. De Bernardo M, Vitiello L, Battipaglia M, et al. Choroidal structural evaluation in celiac disease. *Sci Rep*. 2021;11, 16398.
50. de Oliveira Dias JR, Zhang Q, Garcia JM, et al. Natural history of subclinical neovascularization in nonexudative age-related macular degeneration using swept-source OCT angiography. *Ophthalmology*. 2018;125:255–266.
51. Ding X, Li J, Zeng J, et al. Choroidal thickness in healthy Chinese subjects. *Invest Ophthalmol Vis Sci*. 2011;52:9555–9560.
52. Dolz-Marco R, Glover JP, Gal-Or O, et al. Choroidal and sub-retinal pigment epithelium caverns: multimodal imaging and correspondence with Friedman lipid globules. *Ophthalmology*. 2018;125:1287–1301.
53. Ellabban AA, Tsujikawa A, Ogino K, et al. Choroidal thickness after intravitreal ranibizumab injections for choroidal neovascularization. *Clin Ophthalmol*. 2012:837–844.
54. Esmaeelpour M, Kajic V, Zabihian B, et al. Choroidal Haller's and Sattler's layer thickness measurement using 3-dimensional 1060-nm optical coherence tomography. *PloS One*. 2014;9, e99690.
55. Esser S, Wolburg K, Wolburg H, et al. Vascular endothelial growth factor induces endothelial fenestrations in vitro. *J Cell Biol*. 1998;140:947–959.
56. Farazdaghi MK, Ebrahimi KB. Role of the choroid in age-related macular degeneration: a current review. *J Ophthalmic Vis Res*. 2019.
57. Fein J, Branchini L, Manjunath V, et al. Analysis of short-term change in subfoveal choroidal thickness in eyes with age-related macular degeneration using optical coherence tomography. *Ophthalmic Surg Lasers Imaging Retin*. 2014.
58. Fenner BJ, Cheung CMG, Sim SS, et al. Evolving treatment paradigms for PCV. *Eye*. 2022;36:257–265.
59. Fleckenstein M, Mitchell P, Freund KB, et al. The progression of geographic atrophy secondary to age-related macular degeneration. *Ophthalmology*. 2018;125:369–390.
60. Fragiotta S, Scuderi L, Iodice CM, et al. Choroidal vasculature changes in age-related macular degeneration: from a molecular to a clinical perspective. *Int J Mol Sci*. 2022.
61. Freund KB, Zweifel SA, Engelbert M. Do we need a new classification for choroidal neovascularization in age-related macular degeneration? *LWW*. 2010;30:1333–1349.
62. Friberg TR, Bilonick RA, Brennen PM. Analysis of the relationship between drusen size and drusen area in eyes with age-related macular degeneration. *Ophthalmic Surg Lasers Imaging*. 2011;42:369–375.
63. Fujiwara A, Shiragami C, Shirakata Y, et al. Enhanced depth imaging spectral-domain optical coherence tomography of subfoveal choroidal thickness in normal Japanese eyes. *Jpn J Ophthalmol*. 2012;56:230–235.
64. Fujiwara A, Morizane Y, Hosokawa M, et al. Factors affecting choroidal vascular density in normal eyes: quantification using en face swept-source optical coherence tomography. *Am J Ophthalmol*. 2016;170:1–9.
65. Fukuda Y, Notomi S, Shiose S, et al. Differences in central and peripheral choroidal thickness among the subtypes of age-related macular degeneration in an asian population. *J Clin Med*. 2023;12:5364.
66. Furino C, Boscia F, Reibaldi M, Alessio G. Intravitreal therapy for diabetic macular edema: an update. *J Ophthalmol*. 2021.
67. Gao SS, Jia Y, Zhang M, et al. Optical Coherence Tomography Angiography. *Invest Ophthalmol Vis Sci*. 2016;57(Oct27-36).
68. Giannaccare G, Pellegrini M, Sebastiani S, et al. Choroidal vascularity index quantification in geographic atrophy using binarization of enhanced-depth imaging optical coherence tomographic scans. *Retina*. 2020;40:960–965.
69. Gong J, Yu S, Gong Y, Wang F, Sun X. The diagnostic accuracy of optical coherence tomography angiography for neovascular age-related macular degeneration: a comparison with fundus fluorescein angiography. *J Ophthalmol*. 2016.

70. Greig EC, Moult EM, Despotovic IN, et al. Assessment of choriocapillaris flow prior to nascent geographic atrophy development using optical coherence tomography angiography. *Invest Ophthalmol Vis Sci*. 2024;65:33.
71. Grunwald JE, Hariprasad SM, DuPont J, et al. Foveolar choroidal blood flow in age-related macular degeneration. *Invest Ophthalmol Vis Sci*. 1998;39:385–390.
72. Guo X, Zhou Y, Gu C, et al. Characteristics and classification of choroidal caverns in patients with various retinal and chorioretinal diseases. *J Clin Med*. 2022;11:6994.
73. Heiferman MJ, Fawzi AA. Progression of subclinical choroidal neovascularization in age-related macular degeneration. *PLoS One*. 2019;14, e0217805.
74. Hejun C, Zhang X, Shi X. Ocular changes during hemodialysis in patients with end-stage renal disease. *BMC Ophthalmol*. 2018.
75. Hirahara S, Yasukawa T, Kominami A, Nozaki M, Ogura Y. Densitometry of choroidal vessels in eyes with and without central serous chorioretinopathy by wide-field indocyanine green angiography. *Am J Ophthalmol*. 2016;166:103–111.
76. Hirata M, Tsujikawa A, Matsumoto A, et al. Macular choroidal thickness and volume in normal subjects measured by swept-source optical coherence tomography. *Invest Ophthalmol Vis Sci*. 2011;52:4971–4978.
77. Hollaus M, Iby J, Brugger J, et al. Influence of drusenoid pigment epithelial detachments on the progression of age-related macular degeneration and visual acuity. *Can J Ophthalmol*. 2024.
78. Holz FG, Sheraidah G, Pauleikhoff D, Bird AC. Analysis of lipid deposits extracted from human macular and peripheral Bruch's membrane. *Arch Ophthalmol*. 1994;112:402–406.
79. Hong YJ, Makita S, Jaillon F, et al. High-penetration swept source Doppler optical coherence angiography by fully numerical phase stabilization. *Opt Express*. 2012;20:2740–2760.
80. Hosseini H, Nilforushan N, Moghimi S, et al. Peripapillary and macular choroidal thickness in glaucoma. *J Ophthalmic Vis Res*. 2014;9:154–161.
81. Ibrahim MN, Selvam A, Arora S, et al. Improved 3D Modeling of choroidal Haller's sublayer vasculature based on swept-source OCT scans using Phansalkar thresholding. *Invest Ophthalmol Vis Sci*. 2023;64:1131.
82. Ibrahim MN, Bashar SB, Rasheed MA, et al. Volumetric quantification of choroid and Haller's sublayer using OCT scans: an accurate and unified approach based on stratified smoothing. *Comput Med Imaging Graph*. 2022;99, 102086.
83. Ikuno Y, Kawaguchi K, Nouchi T, Yasuno Y. Choroidal thickness in healthy Japanese subjects. *Invest Ophthalmol Vis Sci*. 2010;51:2173–2176.
84. Invernizzi A, Benatti E, Cozzi M, et al. Choroidal structural changes correlate with neovascular activity in neovascular age related macular degeneration. *Invest Ophthalmol Vis Sci*. 2018;59:3836–3841.
85. Iovino C, Pellegrini M, Bernabei F, et al. Choroidal vascularity index: an in-depth analysis of this novel optical coherence tomography parameter. *J Clin Med*. 2020;9.
86. Jia Y, Tan O, Tokayer J, et al. Split-spectrum amplitude-decorrelation angiography with optical coherence tomography. *Opt Express*. 2012;20:4710–4725.
87. Jia Y, Bailey ST, Hwang TS, et al. Quantitative optical coherence tomography angiography of vascular abnormalities in the living human eye. *Proc Natl Acad Sci USA*. 2015;112:E2395–E2402.
88. Jia Y, Bailey ST, Wilson DJ, et al. Quantitative optical coherence tomography angiography of choroidal neovascularization in age-related macular degeneration. *Ophthalmology*. 2014;121:1435–1444.
89. Jirarattanasopa P, Ooto S, Nakata I, et al. Choroidal thickness, vascular hyperpermeability, and complement factor H in age-related macular degeneration and polypoidal choroidal vasculopathy. *Invest Ophthalmol Vis Sci*. 2012;53:3663–3672.
90. Jonas JB, Forster TM, Steinmetz P, Schlichtenbrede FC, Harder B. Choroidal thickness in age-related macular degeneration. *Retina*. 2014.
91. Kajić V, Esmaeelpour M, Považay B, et al. Automated choroidal segmentation of 1060 nm OCT in healthy and pathologic eyes using a statistical model. *Biomed Opt Express*. 2012;3:86–103.
92. Kanadani TCM, Veloso CE, Nehemy MB. Subfoveal choroidal thickness in eyes with neovascular age-related macular degeneration treated with anti-vascular endothelial growth factor agents. *Ophthalmologica*. 2018;240:200–207.
93. Karslioglu MZ, Kesim C, Yucel O, et al. Choroidal vascularity index in pseudoexfoliative glaucoma. *Int Ophthalmol*. 2021;41:4197–4208.
94. Kim JH, Kim JR, Kang SeW, Kim SJ, Ha HS. Thinner choroid and greater drusen extent in retinal angiomatous proliferation than in typical exudative age-related macular degeneration. e742 *Am J Ophthalmol*. 2013;155:743–749.
95. Kim JM, Cho HJ, Kim Y, et al. *Responses of types 1 and 2 neovascularization in age-related macular degeneration to anti-vascular endothelial growth factor treatment: optical coherence tomography angiography analysis: Seminars in Ophthalmology*. 34. Taylor & Francis; 2019:168–176.
96. Ko AC, Cao S, Pakzad-Vaezi K, et al. Optical coherence tomography–based correlation between choroidal thickness and drusen load in dry age-related macular degeneration. *Retina*. 2013.
97. Koh LHL, Agrawal R, Khandelwal N, Sai Charan L, Chhablani J. Choroidal vascular changes in age-related macular degeneration. *Acta Ophthalmol*. 2017;95:e597–e601.
98. Koizumi H, Yamagishi T, Yamazaki T, Kinoshita S. Relationship between clinical characteristics of polypoidal choroidal vasculopathy and choroidal vascular hyperpermeability. e301 *Am J Ophthalmol*. 2013;155:305–313.
99. Koizumi H, Iida T, Saito M, Nagayama D, Maruko I. Choroidal circulatory disturbances associated with retinal angiomatous proliferation on indocyanine green angiography. *Graefe'S Arch Clin Exp Ophthalmol*. 2008;246:515–520.
100. Koizumi H, Yamagishi T, Yamazaki T, Kawasaki R, Kinoshita S. Subfoveal choroidal thickness in typical age-related macular degeneration and polypoidal choroidal vasculopathy. *Graefes Arch Clin Exp Ophthalmol*. 2011;249:1123–1128.
101. Krytkowska E, Grabowicz A, Mozolewska-Piotrowska K, et al. The impact of vascular risk factors on the thickness and volume of the choroid in AMD patients. *Sci Rep*. 2021;11, 15106.
102. Kuehlewein L, Sadda S, Sarraf D. OCT angiography and sequential quantitative analysis of type 2 neovascularization after ranibizumab therapy. *Eye*. 2015;29:932–935.
103. Kwak JH, Park WK, Kim RY, et al. Unaffected fellow eye neovascularization in patients with type 3 neovascularization: incidence and risk factors. *PLoS One*. 2021;16, e0254186.
104. Lee A, Ra H, Baek J. Choroidal vascular densities of macular disease on ultra-widefield indocyanine green angiography. *Graefe'S Arch Clin Exp Ophthalmol*. 2020;258:1921–1929.
105. Lee B, Ahn J, Yun C, Kim S-W, Oh J. Variation of retinal and choroidal vasculatures in patients with age-related macular degeneration. *Invest Ophthalmol Vis Sci*. 2018;59:5246–5255.
106. Lee H, Kim S, Kim MA, et al. Integrative analysis of the choroid by quantifying Haller vessel and choriocapillaris parameters in different drusen subtypes. *Sci Rep*. 2021;11, 15509.
107. Lee J, Byeon SH. Prevalence and clinical characteristics of pachydrusen in polypoidal choroidal vasculopathy: multimodal image study. *Retina*. 2019;39:670–678.
108. Lee K, Park J-H, Park YG, Park Y-H. Analysis of choroidal thickness and vascularity in patients with unilateral polypoidal choroidal vasculopathy. *Graefe'S Arch Clin Exp Ophthalmol*. 2020;258:1157–1164.
109. Legocki AT, Adhi M, Weber ML, Duker JS. Choroidal morphology and vascular analysis in eyes with neovascular age-related macular degeneration using spectral-domain optical coherence tomography. *Ophthalmic Surg, Lasers Imaging Retin*. 2016;47:618–625.
110. Li J, Liu Z, Lu J, et al. Decreased macular choriocapillaris perfusion in eyes with macular reticular pseudodrusen imaged with swept-source OCT angiography. *Invest Ophthalmol Vis Sci*. 2023;64:15.
111. Li JQ, Welchowski T, Schmid M, et al. Prevalence and incidence of age-related macular degeneration in Europe: a systematic review and meta-analysis. *Br J Ophthalmol*. 2020;104:1077–1084.
112. Li XQ, Larsen M, Munch IC. Subfoveal choroidal thickness in relation to sex and axial length in 93 Danish university students. *Invest Ophthalmol Vis Sci*. 2011;52:8438–8441.
113. Li Z, Hu Y, Cui D, et al. Change in subfoveal choroidal thickness secondary to orthokeratology and its cessation: a predictor for the change in axial length. *Acta Ophthalmol*. 2018.
114. Lim LW, Tan CS, Ting DS. Comparison of polypoidal choroidal vasculopathy lesion sizes measured on multicolor imaging and indocyanine green angiography. *Transl Vis Sci Technol*. 2021.
115. Lindner M, Bezatis A, Czauderna J, et al. Choroidal thickness in geographic atrophy secondary to age-related macular degeneration. *Invest Ophthalmol Vis Sci*. 2015;56:875–882.
116. Lupidi M, Cerquaglia A, Chhablani J, et al. Optical coherence tomography angiography in age-related macular degeneration: The game changer. *Eur J Ophthalmol*. 2018;28:349–357.
117. Lutty GA, McLeod DS, Bhutto IA, Edwards MM, Seddon JM. Choriocapillaris dropout in early age-related macular degeneration. *Exp eye Res*. 2020;192, 107939.
118. Manjunath V, Taha M, Fujimoto JG, Duker JS. Choroidal thickness in normal eyes measured using Cirrus HD optical coherence tomography. e321 *Am J Ophthalmol*. 2010;150:325–329.
119. Manjunath V, Goren J, Fujimoto JG, Duker JS. Analysis of choroidal thickness in age-related macular degeneration using spectral-domain optical coherence tomography. *Am J Ophthalmol*. 2011;152:663–668.
120. Margolis R, Spaide RF. A pilot study of enhanced depth imaging optical coherence tomography of the choroid in normal eyes. *Am J Ophthalmol*. 2009;147:811–815.
121. Maruko I, Iida T, Sugano Y, Furuta M, Sekiryu T. One-year choroidal thickness results after photodynamic therapy for central serous chorioretinopathy. *Retina*. 2011;31:1921–1927.
122. Maruko I, Iida T, Saito M, Nagayama D, Saito K. Clinical characteristics of exudative age-related macular degeneration in Japanese patients. e12 *Am J Ophthalmol*. 2007;144:15–22.
123. Maruko I, Iida T, Sugano Y, Saito M, Sekiryu T. Subfoveal retinal and choroidal thickness after verteporfin photodynamic therapy for polypoidal choroidal vasculopathy. e591 *Am J Ophthalmol*. 2011;151:594–603.
124. Mathis T, Holz FG, Sivaprasad S, et al. Characterisation of macular neovascularisation subtypes in age-related macular degeneration to optimise treatment outcomes. *Eye*. 2023;37:1758–1765.
125. Matsumoto H, Hoshino J, Mukai R, et al. Vortex vein anastomosis at the watershed in pachychoroid spectrum diseases. *Ophthalmol Retin*. 2020;4:938–945.
126. McLeod D.S., Grebe R., Bhutto I.A., et al.: Relationship Between RPE and Choriocapillaris in Age-Related Macular Degeneration. Investigative Opthalmology & Visual Science, 2009.
127. Metrangolo C, Donati S, Mazzola M, et al. OCT biomarkers in neovascular age-related macular degeneration: a narrative review. *J Ophthalmol*. 2021;2021:9994098.
128. Miere A, Butori P, Cohen SY, et al. Vascular remodeling of choroidal neovascularization after ANTI–VASCULAR endothelial growth factor therapy visualized on optical coherence tomography angiography. *Retina*. 2019;39:548–557.
129. Miyake M, Ooto S, Yamashiro K, et al. Pachychoroid Neovasculopathy and Age-Related Macular Degeneration. *Sci Rep*. 2015.

130. Moir J, Kaufmann G, Rodriguez SH, et al. Racial differences in choroidal vascularity index in healthy patients: novel insights. ophthalmic surg lasers imaging. *Retina*. 2024;55:30–38.
131. Muakkassa NW, Chin AT, De Carlo T, et al. Characterizing the effect of anti-vascular endothelial growth factor therapy on treatment-naive choroidal neovascularization using optical coherence tomography angiography. *Retina*. 2015;35:2252–2259.
132. Nagai N, Mushiga Y, Ozawa Y. Retinal pigment epithelial abnormality and choroidal large vascular flow imbalance are associated with choriocapillaris flow deficits in age-related macular degeneration in fellow eyes. *J Clin Med*. 2023.
133. Nakano Y, Kataoka K, Takeuchi J, et al. Vascular maturity of type 1 and type 2 choroidal neovascularization evaluated by optical coherence tomography angiography. *PloS One*. 2019;14, e0216304.
134. Nam J, Nivison-Smith L, Trinh M. Spatial analysis reveals vascular changes in retinal and choroidal vessel perfusion in intermediate AMD with reticular pseudodrusen. *Invest Ophthalmol Vis Sci*. 2024;65:33-33.
135. Nattagh K, Zhou H, Rinella N, et al. OCT angiography to predict geographic atrophy progression using choriocapillaris flow void as a biomarker. *Transl Vis Sci Technol*. 2020;9:6.
136. Neto CAM, Moult EM, Fujimoto JG, Waheed NK, Ferrara D. Choriocapillaris loss in advanced age-related macular degeneration. *J Ophthalmol*. 2018.
137. Nickla DL, Wallman J. The multifunctional choroid. *Prog Retin Eye Res*. 2010;29:144–168.
138. Nomura Y, Takahashi H, Tan X, Obata R, Yanagi Y. Widespread choroidal thickening and abnormal midperipheral fundus autofluorescence characterize exudative age-related macular degeneration with choroidal vascular hyperpermeability. *Clin Ophthalmol 9*. 2015:297–304.
139. Noori J, Esfahani MR, Hajizadeh F, Zaferani M-M. Choroidal mapping; a novel approach for evaluating choroidal thickness and volume. *J Ophthalmic Vis Res*. 2012;7:180.
140. Padrón-Pérez N, Arias L, Rubio M, et al. Changes in choroidal thickness after intravitreal injection of anti-vascular endothelial growth factor in pachychoroid neovasculopathy. *Invest Opthalmology Vis Sci*. 2018.
141. Patel PN, Sheth V. New and innovative treatments for neovascular age-related macular degeneration (nAMD). *J Clin Med*. 2021.
142. Pellegrini M, Bernabei F, Mercanti A, et al. Short-term choroidal vascular changes after aflibercept therapy for neovascular age-related macular degeneration. *Graefes Arch Clin Exp Ophthalmol*. 2021;259:911–918.
143. Povazay B, Hermann B, Hofer B, et al. Wide-field optical coherence tomography of the choroid in vivo. *Invest Ophthalmol Vis Sci*. 2009;50:1856–1863.
144. Querques G, Srour M, Massamba N, et al. Functional characterization and multimodal imaging of treatment-naive "quiescent" choroidal neovascularization. *Invest Ophthalmol Vis Sci*. 2013;54:6886–6892.
145. Querques G, Costanzo E, Miere A, Capuano V, Souied EH. Choroidal caverns: a novel optical coherence tomography finding in geographic atrophy. *Invest Ophthalmol Vis Sci*. 2016;57:2578–2582.
146. Ra H, Jung Y, Lee SH, et al. Quantification of choroidal vascular hyperpermeability on ultra-widefield indocyanine green angiography in macular neovascularization. *Diagnostics*. 2024;14:754.
147. Rahman W, Chen FK, Yeoh J, et al. Repeatability of manual subfoveal choroidal thickness measurements in healthy subjects using the technique of enhanced depth imaging optical coherence tomography. *Invest Ophthalmol Vis Sci*. 2011;52:2267–2271.
148. Ramrattan RS, van der Schaft TL, Mooy CM, et al. Morphometric analysis of Bruch's membrane, the choriocapillaris, and the choroid in aging. *Invest Ophthalmol Vis Sci*. 1994;35:2857–2864.
149. Razavi S, Souied EH, Darvizeh F, Querques G. Assessment of choroidal topographic changes by swept-source optical coherence tomography after intravitreal ranibizumab for exudative age-related macular degeneration. *Am J Ophthalmol*. 2015;160:1006–1013.
150. Rispoli M, Cennamo G, Di Antonio L, et al. Practical guidance for imaging biomarkers in exudative age-related macular degeneration. *Surv Ophthalmol*. 2023.
151. Robbins CB, Grewal DS, Thompson AC, et al. Choroidal structural analysis in Alzheimer disease, mild cognitive impairment, and cognitively healthy controls. *Am J Ophthalmol*. 2021;223:359–367.
152. Rosa R, Corazza P, Musolino M, et al. Choroidal changes in intermediate age-related macular degeneration patients with drusen or pseudodrusen. *Eur J Ophthalmol*. 2021;31:505–513.
153. Rosenfeld PJ, Shen M, Trivizki O, et al. Rediscovering age-related macular degeneration with swept-source OCT imaging: The 2022 Charles L. Schepens, MD, Lecture. *Ophthalmol Retin*. 2024.
154. Ruiz-Medrano J, Ruiz-Moreno JM, Goud A, et al. Age-related changes in choroidal vascular density of healthy subjects based on image binarization of swept-source optical coherence tomography. *Retina*. 2018;38:508–515.
155. Ryu G, Moon C, Hemert Jv, Sagong M. Quantitative analysis of choroidal vasculature in polypoidal choroidal vasculopathy using ultra-widefield indocyanine green angiography. *Sci Rep*. 2020.
156. Sacconi R, Brambati M, Miere A, et al. Characterisation of macular neovascularisation in geographic atrophy. *Br J Ophthalmol*. 2022;106:1282–1287.
157. Sacconi R, Battista M, Borrelli E, et al. Choroidal vascularity index is associated with geographic atrophy progression. *Retina*. 2022.
158. Sacconi R, Vella G, Battista M, et al. Choroidal vascularity index in different cohorts of dry age-related macular degeneration. *Transl Vis Sci Technol*. 2021;10:26-26.
159. Sacconi R, Forte P, Capuano V, et al. Optical coherence tomography angiography characterization of evolving lesions in fellow eyes of exudative type 3 macular neovascularization patients. *Retina*. 2022;42:2075–2082.
160. Sacconi R, Forte P, Tombolini B, et al. OCT predictors of 3-year visual outcome for type 3 macular neovascularization. *Ophthalmol Retin*. 2022;6:586–594.
161. Sacconi R, Sarraf D, Garrity S, et al. Nascent type 3 neovascularization in age-related macular degeneration. *Ophthalmol Retin*. 2018;2:1097–1106.
162. Sakurada Y, Leong BCS, Parikh R, Fragiotta S, Freund KB. Association between choroidal caverns and choroidal vascular hyperpermeability in eyes with pachychoroid diseases. *RETINA*. 2018;38:1977–1983.
163. Sánchez-Cano A, Orduna E, Segura F, et al. Choroidal thickness and volume in healthy young white adults and the relationships between them and axial length, ammetropy and sex. *Am J Ophthalmol*. 2014.
164. Sasahara M, Tsujikawa A, Musashi K, et al. Polypoidal choroidal vasculopathy with choroidal vascular hyperpermeability. e601 *Am J Ophthalmol*. 2006;142:601–607.
165. Sato Y, Ueda-Arakawa N, Takahashi A, et al. Clinical characteristics and progression of geographic atrophy in a japanese population. *Ophthalmol Retin*. 2023.
166. Scharf JM, Corradetti G, Alagorie AR, et al. Choriocapillaris flow deficits and treatment-naïve macular neovascularization secondary to age-related macular degeneration. *Invest Ophthalmol Vis Sci*. 2020;61:11-11.
167. Schmitz-Valckenberg S, Sadda SR, Staurenghi G, et al. Geographic Atrophy. *Retina*. 2016.
168. Schwartz DM, Fingler J, Kim DY, et al. Phase-variance optical coherence tomography: a technique for noninvasive angiography. *Ophthalmology*. 2014;121:180–187.
169. Shen M, Zhou H, Lu J, et al. Choroidal changes after Anti-VEGF therapy in amd eyes with different types of macular neovascularization using swept-source OCT angiography. *Invest Ophthalmol Vis Sci*. 2023;64:16.
170. Sheth J, Anantharaman G, Kumar N, et al. Pachydrusen: the epidemiology of pachydrusen and its relevance to progression of pachychoroid disease spectrum. *Eye (Lond)*. 2020;34:1501–1503.
171. Shin JY, Kwon KY, Byeon SH. Association between choroidal thickness and the response to intravitreal ranibizumab injection in age-related macular degeneration. *Acta Ophthalmol*. 2015;93:524–532.
172. Singh SR, Invernizzi A, Rasheed MA, et al. Wide-field choroidal vascularity in healthy eyes. *Am J Ophthalmol*. 2018;193:100–105.
173. Singh SR, Vupparaboina KK, Goud A, Dansingani KK, Chhablani J. Choroidal imaging biomarkers. *Surv Ophthalmol*. 2019;64:312–333.
174. Singh SR, Oli A, Mohan S, et al. Pachydrusen in Indian population: a hospital-based study. *Indian J Ophthalmol*. 2019;67:371–375.
175. Sonoda S, Sakamoto T, Yamashita T, et al. Luminal and stromal areas of choroid determined by binarization method of optical coherence tomographic images. e1121 *Am J Ophthalmol*. 2015;159:1123–1131.
176. Spaide RF. Disease expression in nonexudative age-related macular degeneration varies with choroidal thickness. *Retina*. 2018;38:708–716.
177. Spaide RF, Koizumi H, Pozonni MC. Enhanced depth imaging spectral-domain optical coherence tomography. *Am J Ophthalmol*. 2008;146:496–500.
178. Srinath N, Patil A, Kumar VK, et al. Automated detection of choroid boundary and vessels in optical coherence tomography images. *Annu Int Conf IEEE Eng Med Biol Soc*. 2014;2014:166–169.
179. Sunil Ganekal VG. Correlation between choroidal vascularity index, flow pattern and neovascular activity in treatment naive eyes of age related macular degeneration. *Indian J Clin Exp Ophthalmol*. 2022;8:198–203.
180. Taibouni K, Mière A, Samake A, et al. Choroidal neovascularization screening on OCT-angiography choriocapillaris images by convolutional neural networks. *Appl Sci*. 2021.
181. Tanaka A, Hata M, Tsuchikawa M, et al. Short-term outcomes of 3 monthly intravitreal faricimab on different subtypes of neovascular age-related macular degeneration. *Clin Ophthalmol*. 2024;18:507–516.
182. Temel E, Aşıkgarip N, Koçak Y, et al. Analysis of choroidal vascularity index in multiple sclerosis patients without optic neuritis attack. *Photo Photo Ther*. 2022;38,102823.
183. Thomas CJ, Mirza RG, Gill MK. Age-related macular degeneration. *Med Clin*. 2021;105:473–491.
184. Thorell MR, Goldhardt R, Nunes RP, et al. Association between subfoveal choroidal thickness, reticular pseudodrusen, and geographic atrophy in age-related macular degeneration. *Ophthalmic Surg, Lasers Imaging Retin*. 2015;46:513–521.
185. Ting DS, Ng WY, Ng SR, et al. Choroidal thickness changes in age-related macular degeneration and polypoidal choroidal vasculopathy: a 12-month prospective study. *Am J Ophthalmol*. 2016;164(128-136), e121.
186. Tombolini B., Crincoli E., Sacconi R., et al.: Optical Coherence Tomography Angiography: A 2023 Focused Update on Age-Related Macular Degeneration. Ophthalmology and Therapy:1-19, 2024.
187. Uppugunduri SR, Rasheed MA, Richhariya A, et al. Automated quantification of Haller's layer in choroid using swept-source optical coherence tomography. *PLoS One*. 2018;13, e0193324.
188. Uyar E, Dogan U, Ulas F. Çelebi S: Effect of fasting on choroidal thickness and its diurnal variation. *Curr Eye Res*. 2019;44:695–700.
189. Uzun S, Uzun F. Choroid and choriocapillaris changes in early-stage Parkinson's disease: a swept-source optical coherence tomography angiography-based cross-sectional study. *Alzheimers Res Ther*. 2023;15:35.
190. Valsecchi N, Roda M, Febbraro S, et al. Choroidal morphology and microvascular structure in eyes of patients with idiopathic normal pressure hydrocephalus before and after ventriculo-peritoneal shunt surgery. *Sci Rep*. 2023;13, 16379.
191. VanDenLangenberg A.M., Carson M.P.: Drusen Bodies. 2020.

192. Vincent SJ, Collins MJ, Read SA, Carney LG. Retinal and Choroidal Thickness in Myopic Anisometropia. *Invest Opthalmol Vis Sci*. 2013.
193. Vupparaboina KK, Nizampatnam S, Chhablani J, Richhariya A, Jana S. Automated estimation of choroidal thickness distribution and volume based on OCT images of posterior visual section. *Comput Med Imaging Graph*. 2015;46(Pt 3):315–327.
194. Vupparaboina KK, Dansingani KK, Goud A, et al. Quantitative shadow compensated optical coherence tomography of choroidal vasculature. *Sci Rep*. 2018;8:6461.
195. Vyas CH, Cheung CMG, Jordan-Yu JMN, et al. Novel volumetric imaging biomarkers for assessing disease activity in eyes with PCV. *Sci Rep*. 2022;12:2993.
196. Waheed N.K., Moult E.M., Fujimoto J.G., Rosenfeld P.J.: Optical Coherence Tomography Angiography of Dry Age-Related Macular Degeneration. 2016.
197. Wang W-Q, Wang F, Qin W, et al. Joint antiangiogenic effect of ATN-161 and anti-vegf antibody in a rat model of early wet age-related macular degeneration. *Mol Pharm*. 2016.
198. Wei X, Ting DSW, Ng WY, et al. Choroidal vascularity index: a novel optical coherence tomography based parameter in patients with exudative age-related macular degeneration. *Retina*. 2017;37:1120–1125.
199. Wells J.A., Glassman A.R., Ayala A.R., et al.: Aflibercept, Bevacizumab, or Ranibizumab for Diabetic Macular Edema. New England Journal of Medicine, 2015.
200. Wu Z, Zhou X, Chu Z, et al. Impact of reticular pseudodrusen on choriocapillaris flow deficits and choroidal structure on optical coherence tomography angiography. *Invest Ophthalmol Vis Sci*. 2022;63:1.
201. Xu D, Dávila JP, Rahimi M, et al. Long-term progression of type 1 neovascularization in age-related macular degeneration using optical coherence tomography angiography. *Am J Ophthalmol*. 2018;187:10–20.
202. Yamazaki T, Koizumi H, Yamagishi T, Kinoshita S. Subfoveal choroidal thickness in retinal angiomatous proliferation. *Retina*. 2014;34:1316–1322.
203. Yamazaki T, Koizumi H, Yamagishi T, Kinoshita S. Subfoveal choroidal thickness after ranibizumab therapy for neovascular age-related macular degeneration: 12-Month Results. *Ophthalmology*. 2012;119:1621–1627.
204. Yanagi Y, Ting DSW, Ng WY, et al. Choroidal vascular hyperpermeability as a predictor of treatment response for polypoidal choroidal vasculopathy. *Retina*. 2018;38:1509–1517.
205. Yannuzzi LA, Wong DWK, Sforzolini BS, et al. Polypoidal choroidal vasculopathy and neovascularized age-related macular degeneration. *Arch Ophthalmol*. 1999.
206. Yeo NJY, Chan EJJ, Cheung C. Choroidal neovascularization: mechanisms of endothelial dysfunction. *Front Pharmacol*. 2019;10:1363.
207. Yiu G, Chiu SJ, Petrou PA, et al. Relationship of central choroidal thickness with age-related macular degeneration status. e612 *Am J Ophthalmol*. 2015;159:617–626.
208. Yiu G, Manjunath V, Chiu SJ, Farsiu S, Mahmoud TH. Effect of anti–vascular endothelial growth factor therapy on choroidal thickness in diabetic macular edema. *Am J Ophthalmol*. 2014.
209. Yoon JM, Shin DH, Kong M, Ham D-I. Age-related macular degeneration eyes presenting with cuticular drusen and reticular pseudodrusen. *Sci Rep*. 2022;12:5681.
210. Yuzawa M, Mori R, Kawamura A. The origins of polypoidal choroidal vasculopathy. *Br J Ophthalmol*. 2005;89:602–607.
211. Zhang L, Lee K, Niemeijer M, et al. Automated segmentation of the choroid from clinical SD-OCT. *Invest Ophthalmol Vis Sci*. 2012;53:7510–7519.